Thermal Conductivity and Thermal Diffusivity of Liquid Copper

DIPLOMA THESIS

Claus Cagran

Institut für Experimentalphysik
February 2000

Technische Universität
Graz

Meinen Eltern, meinen beiden Brüdern und
Angelika gewidmet.

Abstract

A general survey of different thermophysical measurement-methods is given within this work, focusing mainly on techniques, which are used to determine thermal conductivity and thermal diffusivity of metals and alloys both in the solid state, as well as at the melting point and into the liquid phase. By using a subsecond ohmic pulse-heating technique it is possible to measure thermophysical properties of metals and alloys at temperature regions that are inaccesible to most other techniques. This technique enables heating rates up to 10^8 K/s and thus is applied for short time (µs) measurements of thermophysical properties of electrical conducting materials. Because of the short time of the experiments no chemical interactions between the sample and its environment occur. Using pulse-heating, measurements on wire-shaped Copper (Cu) specimens of 0.5 mm diameter and an average length of 50 mm were performed and the results - especially thermal conductivity and thermal diffusivity up to 500 K into the liquid phase - are discussed and compared to literature values.

In der vorliegenden Arbeit wird ein genereller Überblick über verschiedene Methoden zur Messung thermophysikalischer Daten von Metallen und Legierungen gegeben. Ganz besonderes Augenmerk wurde dabei auf Techniken gelegt, die eine Messung der Wärmeleitfähigkeit und der Temperaturleitfähigkeit - sowohl von Festkörpern als auch von Flüssigkeiten - ermöglichen. Eine dieser Methoden ist die Ohm'sche Pulsheizung elektrisch leitender Materialien, die eine Ermittlung der thermophysikalischen Daten bis in Temperaturbereiche erlaubt, die mit herkömmlichen Techniken (z.B. Messungen im oder nahe dem thermodynamischen Gleichgewicht) nicht erreicht werden können. Damit werden Aufheizraten bis zu 10^8 K/s erreicht, wodurch Messungen im µs-Bereich ermöglicht und chemische Wechselwirkungen mit der Umgebung nahezu ausgeschlossen werden können. In dieser Arbeit wurden Messungen an hochreinen (99,996 %) Kupferdrähten (Cu) mit einem Durchmesser von 0,5 mm und einer durchschnittlichen Länge von 50 mm durchgeführt und die daraus ermittelten Daten - vor allem Wärmeleitfähigkeit und Temperaturleitfähigkeit bis 500 K in die flüssige Phase - diskutiert und mit Literaturwerten verglichen.

Contents

Chapter 1

Introduction

For several years now, the Subsecond Thermophysics Group of the Institute for Experimental Physics performs thermophysical properties measurements by using a ohmic pulse-heating technique. With this technique, good results have been obtained for both, pure metals such as Au, Nb, W, or Ni, as well as for alloys such as Inconel 718 or Invar® (Fe-Ni).
The data obtained by our measurements are of the greatest interest for the metalworking industry, i.e. as input data for computer simulations to model liquid metal processing operations such as casting or welding (MAGMAsoft), to understand and design processing equipment such as facilities for the growth of single crystals from the melt, to obtain more accurate phase diagrams, for better assessment of potential accidents in the design of safer nuclear reactors, for aerospace techniques, or just for fundamental materials research reasons.

This present work deals with the determination of thermal conductivity and thermal diffusivity of pure Copper (Cu). Copper itself has already been measured at the Institute a couple of years ago with good results, but this time we mainly focused on different properties like thermal conductivity and thermal diffusivity. Back in 1993, the pyrometer was able to properly detect the melting-plateau of Copper, although the surface radiation of Copper is low, which is - by using PLANCK's law on black body radiation - a result of the low melting temperature of Copper. By way of contrast, all the signals and data from the solid state before melting were covered by the noise of the amplifying electronic and were therefore inaccessible. As a matter of facts, some quantities such as the enthalpy or the electrical resistivity at the melting transition led to good results, whereas measurements in the solid state were nearly unpracticable.

Meanwhile, this problem has been removed by renewing and improving our apparatus. We have a new interference filter in the pyrometer with a wider bandwith and new amplification electronics with better signal to noise ratio. Therefore we felt able to measure the properties of

Copper again. But we did not think about re-measuring the properties of liquid Copper until we got an inquiry from Dr. John Redgrove, Head of Thermophysical Properties Section, National Physical Laboratory (NPL), London, who have been commissioned to develop a national standard for measurement of the thermal diffusivity and thermal conductivity of molten materials. The objectives of their 3-year project, which began July 1998, are to:

- support the process industries by providing a thermal conductivity/diffusivity measurement standard for molten materials
- provide data on key reference materials.

As a part of the validation, they want to intercompare measurements on selected materials with other laboratories and different measurement techniques to get an estimation of the accuracy of both, the measured values as well as the different techniques. NPL asked us to participate in the intercomparison of about 20 different laboratories worldwide and to contribute the thermophysical properties - mainly the thermal conductivity and the thermal diffusivity - of Copper at 1356 K to 1473 K to their molten materials intercomparison.

Copper itself is commonly used as a reference material because of several reasons: the low and well known melting temperature, good mechanical properties, good electrical properties such as high electrical conductivity (only silver (Ag) has a better electrical conductivity than Copper) and therefore a low resistivity, and of course its availability to name just a few. NPL also aims to publish the final results after the 3 years in the scientific literature to make the data accessible to the scientific community.

Although we knew that the same reasons that make Copper such a good reference material are the ones to make measurements more complicated and difficult, we agreed and participated in the intercomparison project with NPL. Not at least, these new Copper measurements are a quite good indicator for the present abilities of our measurement system.

Chapter 2

Fundamental Theory

2.1 Definitions of thermal conductivity and thermal diffusivity

As a starting point for a short derivation, a cylindrical rod which is isolated against heat losses along the surface is chosen. We look at the heat-transfer parallel to the cylinder-axis.

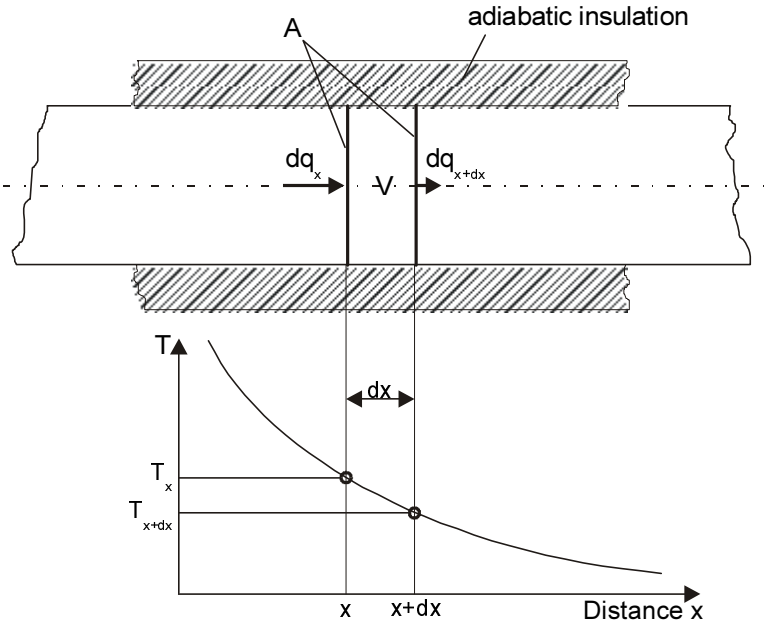

Fig. 1: Schematic displaying the basics of heat conduction. Key: T, temperature; x, distance; dq, heat flux; A, area; V, volume.

Fourier's principle law of the heat-transfer reads:

$$q = -\lambda \cdot gradT \qquad \textbf{2-1}$$

where q is the heat flux, T the temperature and λ the thermal conductivity.

Fourier made the assumption, that the perpendicular heat flow across the unit area A per unit time must be proportional to the unit area A and the temperature gradient -dT/dx, which leads to:

$$\Phi = \frac{dq}{dT} = -\lambda \cdot A \cdot \frac{dT}{dx} \qquad \textbf{2-2}$$

where Φ is the heat current, and A the unit area.

In this equation thermal conductivity λ is a proportional constant. It has to be stated here, that λ itself could be a temperature dependent quantity and therefore could not longer be seen as a constant.

If we make some simple conversions with Eq.(2-2) we find the well known description:

$$\lambda = -\frac{q}{A \cdot \frac{dT}{dx}} \qquad \textbf{2-3}$$

One can see, that thermal conductivity λ can be defined as the heat flux q conducted across an unit area A per second per unit temperature gradient and has the dimension [$Wm^{-1}K^{-1}$].

Similar to the derivation of the equation for diffusion, the entire mathematical solution can only be found, if the temperature T within the cylinder is known as a function of time t and place ***x*** (T(x, y, z, t)). The equation considering those points is known as the differential equation of heat transfer:

$$\frac{dT}{dt} = \frac{\lambda}{d \cdot c_p} \cdot \frac{\partial^2 T}{\partial x^2} \qquad \textbf{2-4}$$

where d is the density and c_p the heat capacity.

Combining the constants from Eq.(2-4), one gets the thermal diffusivity a, which is defined as:

$$a = \frac{\lambda}{d \cdot c_p} \qquad \textbf{2-5}$$

Thermal diffusivity represents the rate of heat diffusion per unit time and has the dimension [m^2s^{-1}]. Eq.(2-4) equals FICK's 2^{nd} law of diffusion, which reflects in the name thermal diffusivity.

As one can see, Eq.(2-5) creates a relation between thermal conductivity and thermal diffusivity. This is very important for different measurements, because in some methods it is not thermal conductivity λ but thermal diffusivity a which is determined, as with the knowledge of one quantity it's possible to determine the other quantity.

2.2 Experimental determination

Before the various different methods used to measure thermal conductivities and diffusivities are discussed in the next chapter, I want to call your attention to two things, which should always be kept in mind while discussing these methods:

- The first point is how convection affects the specific measurement or how one can prevent the effect of convection.

- The second point is the close relationship of thermal conductivity with electrical conductivity. These similarities lead to some totally different possibilities of measuring these quantities.

2.2.1 Convection

When thermal conductivity measurements are carried out on liquids, the heat flux q can obtain substantial contributions from convection and can lead to erroneously high values for thermal conductivity (and also for thermal diffusivity). Consequently, great efforts are made to minimize convection by:

(i) accurate temperature control of the sample
(ii) ensuing that the free surface of the liquid is at marginally higher temperature than that of the base of the sample

However, many metals melt at very high temperatures and in practice it is very difficult to provide the necessary control of temperature under these conditions. Consequently, in recent years transient and non-steady state methods (see Chapter 3) have been increasingly used to

carry out measurements on liquid metals and alloys. In these experiments the measurements are carried out rapidly with a view to complete the entire experiment before the onset of convection.

2.2.2 Relationship of thermal conductivity with electrical conductivity; the WIEDEMANN-FRANZ-Law

In many different practical cases electrical conductivity *(σ)* or electrical resistivity *($1/\sigma$)* measurements are a lot easier to perform than the determination of the thermal conductivity itself; thus, a relation between these values is needed to derive λ either from σ or $1/\sigma$ - the WIEDEMANN-FRANZ-LORENTZ law (WFL). [Klemens and Williams, 1986] have shown it's theoretical derivation, which is summed up on the following pages:

Theory

The thermal conductivity of metals and alloys is composed of two components: a lattice component λ_l and an electronic component λ_e. In both cases heat is transported by mobile carriers, and thermal conductivity due to each carrier can be expressed in the form

$$\lambda_i = \frac{1}{3} \cdot C_i \cdot v_i \cdot l_i \qquad \textbf{2-6}$$

Here C_i is the contribution of carriers of type i to the specific heat per unit volume, v_i is the average speed of those carriers, and l_i their mean free path. This equation has the same form as the expression for thermal conductivity in the kinetic theory of gases, and can be derived from a BOLTZMANN equation. Since the contributions of these two types of carriers could be divided further into subgroups, the overall thermal conductivity becomes the sum of these contributions

$$\lambda = \sum_i \lambda_i \qquad \textbf{2-7}$$

As mentioned before, thermal conduction in metals and alloys consists of a lattice and an electronic component. Several investigators have shown experimentally, that although the mechanism of phonon or lattice conduction can make a significant contribution at lower temperatures, electronic conduction is dominant at temperatures around the melting point [NPL Report, 1997]. With these assumptions theory leads to the WFL by just lookink at the electronic component.

Electronic component - the LORENTZ ratio

Eq.(2-6) holds for the electronic component as well as for the lattice component, but it is more useful to relate λ_e to the electrical conductivity σ. In part, this follows because C_e, the electronic component of the specific heat, is only a small part of the total specific heat, and thus not easily deduced from measurements. The main advantage of expressing λ_e in terms of σ is, that both quantities are directly proportional to the electron mean free path l_e, so that the ratio λ_e/σ is independent of l_e; furthermore σ is relatively easy to measure. This assumes, of course, that the mean free path l_e, as properly defined through a BOLTZMANN equation, is the same for electrical as for thermal conduction. While this is by no means universally true, differences in the two mean free paths are important mainly at low temperatures, where electron scattering is both inelastic and anisotropic.

In the first instance let us assume a mean free path which is the same for electrical and thermal conduction. Each electron is treated as being in a definite state of motion, specified by its momentum ***p***, but having its position completely unspecified within the volume of the solid. For each ***p***-value there are two possible values of spin; the state of the electron is specified by its momentum spin. According to the Pauli exclusion principle, there cannot be more than one electron in each such state. The average number of electrons per state defines the distribution function *f(**p**)*. The electron does not move in free space, but in the periodic potential of the crystal lattice, hence *E(**p**)*, the energy of the electron of the momentum ***p***, differs from that of a free electron.

In a perfectly periodic lattice each electron conserves its momentum value ***p***, as if it would move in free space. Deviations from periodicity (lattice vibrations, imperfections, boundaries) cause electrons to be scattered from one p-state to another unoccupied state. In thermal equilibrium the occupation number attains, in average, the value given by the FERMI-DIRAC distribution $f^0(\mathbf{p})$:

$$f^0(\vec{\mathrm{p}}) = \frac{1}{e^{\frac{(E-\zeta)}{k_B T}} + 1} \qquad \textbf{2-8}$$

where k_B is the BOLTZMANN constant and ζ (the FERMI energy) is similar to a chemical potential and is determined by the electron density.

If the distribution function $f(\mathbf{p})$ departs systematically (i.e. for a large group of states) from its equilibrium value f^0, the same scattering processes will tend to restore the equilibrium distribution. The rate of return towards equilibrium can be characterized by a relaxation time $\tau(\mathbf{p})$: the rate of change of $f(\mathbf{p})$ due to the interaction (int) processes is expressed as

$$\frac{df}{dt}|_{\text{int}} = -\frac{f(\vec{p}) - f^0(\vec{p})}{\tau(\vec{p})} = -\frac{g(\vec{p})}{\tau(\vec{p})} \qquad \textbf{2-9}$$

where $g(\mathbf{p})$ is the departure of the distribution function from its equilibrium value. The mean free path is defined as $l_e = v_e \tau$, where $\mathbf{v_e} = d\mathbf{E}/d\mathbf{p}$ is the electron velocity.

An electric field $\mathbf{F}$ or a temperature gradient $\nabla \mathbf{T}$, will tend to change the distribution function at a rate

$$\frac{df}{dt}|_{F,\nabla T} = -e\vec{F} \cdot \vec{v}_e \frac{df^0}{dE} - \nabla T \cdot \vec{v}_e \frac{df^0}{dT} \qquad \textbf{2-10}$$

where e the electron charge.

The BOLTZMANN equation states that the net rate of change due to equations (2-9) and (2-10) is zero in a steady state, so that

$$g(\vec{p}) = -\tau(\vec{p}) \frac{df^0}{dE} \vec{v}_e \cdot \left[e\vec{F} - k_B \left(\varepsilon + \frac{1}{k_B} \frac{d\zeta}{dT} \right) \nabla T \right] \qquad \textbf{2-11}$$

where $\varepsilon = (E-\zeta)/k_B T$ is the BOLTZMANN term.

In thermal equilibrium the electric current density j and the heat current density Q vanish. Both of these currents thus can be expressed as

$$\begin{aligned} j &= \frac{2e}{h^3} \int \vec{v}_e g(\vec{p}) d\vec{p} \\ Q &= \frac{2}{h^3} \int \vec{v}_e (E - \zeta) g(\vec{p}) d\vec{p} \end{aligned} \qquad \textbf{2-12}$$

since $2h^{-3}d\mathbf{p}$ is the number of quantum states per unit volume in an element $d\mathbf{p}$ of $\mathbf{p}$-space; h is PLANCK's constant.

One now can arrange the integration over p-space in terms of integrating over surfaces of constant energy E in $\boldsymbol{p}$-space, and then over E. Now $dE = k_B T d\varepsilon$. The factor $df^0/dE = (k_B T)^{-1}(df^0/d\varepsilon)$ occurs in both integrals in Eq.(2-12), and $df^0/d\varepsilon$ is an even function of ε. The various terms in equation (2-11) and (2-12) can be grouped according to their power of ε. Retaining terms even in ε we arrive at the following results.

The isothermal electrical conductivity, defined as $\sigma = j/F$ when $\nabla T = 0$, can be written as

$$\sigma = M_0 = \int \sigma(\varepsilon)\left(\frac{df^0}{d\varepsilon}\right)d\varepsilon \qquad \textbf{2-13}$$

and is thus the zero'th moment of a partial conductivity tensor $\sigma_{ij}(\varepsilon)(df^0/d\varepsilon)$ where

$$\sigma_{ij}(\varepsilon) = \frac{2e^2}{h^3}\oint \tau(p) v_i(\vec{p}) v_j(\vec{p}) |v_e(\vec{p})|^{-1} dS \qquad \textbf{2-14}$$

where i, j denote Cartesian components, dS is a surface element of the contour $E(p) = E$ in $\boldsymbol{p}$-space and the integration is over the entire contour $E = k_B T\varepsilon + \zeta$.

One can define the first and second moment of the same partial conductivity by

$$M_n = \int \sigma(\varepsilon)\varepsilon^n\left(\frac{df^0}{d\varepsilon}\right)d\varepsilon \qquad \textbf{2-15}$$

The Peltier coefficient Π is defined as Q/j when $\nabla T = 0$, and one can show that

$$\Pi = \left(\frac{k_B T}{e}\right)\left(\frac{M_1}{M_0}\right) \qquad \textbf{2-16}$$

The electronic component of thermal conductivity is defined as $\lambda_e = -Q/\nabla T$ under the condition j = 0. The latter condition determines the thermoelectric power $S_e = \Pi/T = [F - kB^{-1}(d\zeta/dT)]/\nabla T$ and one finally obtains

$$\lambda_e = \left(\frac{k_B}{e}\right)^2 T\left[\frac{M_2 - M_1^2}{M_0}\right] \qquad \textbf{2-17}$$

The electronic thermal conductivity can be related to the electrical conductivity by the LORENTZ ratio

$$L = \frac{\lambda_e}{\sigma T} = \left(\frac{k_B}{e}\right)^2 \left[\left(\frac{M_2}{M_0}\right) - \left(\frac{M_1}{M_0}\right)^2\right] = \left(\frac{k_B}{e}\right)^2 \left(\frac{M_2}{M_0}\right) - S_e^2 \qquad \textbf{2-18}$$

While Eq.(2-18) holds for semiconductors and semimetals as well as for good metallic conductors, we are particularly interested in the case of high degeneracy, where the electron density is so high and the FERMI energy so large that $\sigma(E)$ can be expanded as a TAYLOR series about ζ:

$$\sigma(E) = \sigma(\zeta) + k_B T \varepsilon \left(\frac{d\sigma}{dE}\right)_\zeta + \frac{1}{2}(k_B T)^2 \varepsilon^2 \left(\frac{d^2\sigma}{dE^2}\right)_\zeta + \ldots \qquad \textbf{2-19}$$

so that electrical conductivity, thermoelectric power, thermal conductivity, and the LORENTZ ratio are given by

$$\sigma = \sigma(\zeta) + \frac{\pi^2}{6}(k_B T)^2 \left(\frac{d^2\sigma(E)}{dE^2}\right)_\zeta \qquad \textbf{2-20}$$

$$S_e = \left(\frac{k_B}{e}\right) \frac{\pi^2}{3}(k_B T) \frac{1}{\sigma} \left(\frac{d\sigma(E)}{dE}\right)_\zeta \qquad \textbf{2-21}$$

$$\lambda_e = L \cdot \sigma \cdot T \qquad \textbf{2-22}$$

and

$$L = \left(\frac{\pi^2}{3}\right)\left(\frac{k_B}{e}\right)^2 + \left(\frac{21\pi^4}{90}\right)\left(\frac{k_B}{e}\right)^2 \times (k_B T)^2 \left(\frac{1}{\sigma}\frac{d^2\sigma(E)}{dE^2}\right)_\zeta - S_e^2 \qquad \textbf{2-23}$$

The leading term in Eq.(2-23), $L_0 = (\pi^2/3)(k_B/e)^2$, is the SOMMERFELD value of the LORENTZ ratio.

Integrals of the type

$$I_n = \int_{-\infty}^{\infty} \varepsilon^n \exp\varepsilon\left(\exp\varepsilon + 1\right)^{-2} d\varepsilon \qquad \textbf{2-24}$$

have been expanded and expressed in terms of the RIEMANN zeta function. Thus, $I_2 = \pi^2/3$, $I_4 = 42\pi^4/90$, and for higher even values of n, $I_n \approx 2(n!)$.

These above relations were derived under the assumption that the relaxation time $\tau(\boldsymbol{p})$ is a function of p, but is independent of the functional form of $g(\boldsymbol{p})$: thus $\tau(\boldsymbol{p})$ is assumed to be the same for electrical and thermal conduction, so that $\sigma(\varepsilon)$ is also unique. In cases when this condition is not satisfied, Eq.(2-23) would not hold, because the magnitude of $\sigma(E)$ would not cancel out in the ratio of moments of Eq.(2-22).

Nevertheless, these results are in good agreement with the experimentally obtained results and used for data evaluation.

2.3 Summary of important equations from the derivation

WIEDEMANN-FRANZ-LORENTZ law (WFL)

Simple manipulations with Eq.(2-22) lead to the WIEDEMANN-FRANZ law (in the description of L. LORENTZ, 1872):

$$L = \frac{\lambda}{\sigma \cdot T} \qquad \text{or} \qquad \lambda = L \cdot \sigma \cdot T \qquad \textbf{2-25}$$

where L is the LORENTZ number, λ is thermal conductivity, σ is electrical conductivity and T is temperature.

LORENTZ number

As mentioned before, the leading term in Eq.(2-23)

$$L = \frac{\pi^2}{3} \cdot \left(\frac{k_B}{e} \right)^2 \qquad \textbf{2-26}$$

is the SOMMERFELD value of the LORENTZ ratio. As we can see, it depends only on constants and - as a matter of facts - is a constant itself. Its universal value can be calculated with the use of some quantum mechanics and should read, [Bergmann-Schaefer, 1990]:

$$L = 2{,}44 \cdot 10^8 \ \frac{V^2}{K^2}$$

Table 1: Electrical conductivities *(σ)* and LORENTZ numbers *(L)* for different metals at different temperatures [Bergmann-Schaefer, 1990]

	Electrical conductivity $\sigma \cdot 10^{-5}$, $[\Omega^{-1}cm^{-1}]$				**LORENTZ number $\lambda/\sigma T \cdot 10^8$, $[V^2/K^2]$**			
Temperature [K]	**80**	**273**	**373**	**573**	**80**	**273**	**373**	**573**
Silver	32,5	6,70	4,76	2,97	1,77	2,28	2,36	2,41
Copper	43,6	6,45	4,50	2,79	1,56	2,24	2,35	2,37
Gold	20,6	4,90	3,51	2,20	2,03	2,35	2,36	2,42
Aluminum	28,8	4,15	2,86	1,80	1,11	2,03	2,11	2,13
Zinc	9,90	2,08	1,47	0,890	1,70	1,90	1,92	1,96
Nickel	9,30	1,65	0,990	0,452	1,68	1,95	2,28	2,43
Platinum	4,95	1,02	0,733	0,476	2,00	2,55	2,60	2,75
Lead	2,02	0,532	0,375	0,224	2,33	2,31	2,40	2,62

Table 1 shows the validity of the WFL for higher (> 273 K) temperatures, although the electrical conductivity values are differing in the range of 10^2. Unfortunately the values for the LORENTZ number are not exact the same as the theoretical value, which leads to a uncertainty while using the WFL for different materials.

Unsurprisingly, as the WFL was derived under omission of the lattice or phonon component of conduction (which is dominant at low temperatures), Table 1 shows the failure of the WFL in the low temperature range.

Chapter 2

Survey of methods

3.1 Classification of methods used to measure thermal conductivity and diffusivity of metals

Most of the techniques used to determine thermal conductivity and thermal diffusivity can be classified into steady state, non-steady state and transient techniques, even though this classification is not always easy and clear. Especially the differences between non-steady state and transient techniques are very small.

- Steady state means a steady temperature gradient across the whole specimen. These techniques require very accurate temperature control throughout to minimize convection. This becomes progressively more difficult as the temperature increases, and consequently these methods have mostly been used on low melting metals such as tin and lead.

- Non-steady state techniques and as well transient techniques have been used with a view to completing the experiments before the onset of convection. In non-steady state experiments this is accomplished by using very high heating rates (up to 1000 Ks^{-1} and above) so the duration of experiments for the liquid phase is < 0,2 second. The methods summed up into this category are historically the first ones to abandon the well known environment of the steady state measurements, but non-steady state experiments became more and more less important as time went on. These days transient techniques and methods are a more powerful and reliable tool for dynamic measurements.

- Transient methods on liquids have indicated that convection occurs after ca. 1 second but the temperature differences in the transient techniques are of the order of 5 K, compared with > 100 K in the non-steady state experiments. These large temperature gradients may give rise to convectional flows due to buoyancy and thermocapillary forces. Thus convectional contributions to the thermal conductivity can not be ruled out in these non-steady state experiments, indeed there are some cases (i.e. Fe) where this appears to have occured. As a matter of facts, transient methods more or less have replaced non-steady state techniques because of the smaller temperature gradients and the better results.

  Transient techniques have become widely used for measurements on organic liquids since the measurement can be carried out rapidly in order to minimize convection. These techniques appear to have a distinct advantage but may be limited in their application to temperatures of less than 1300 K due to the fact that (i) insulators become electrical conductors at high temperatures and (ii) reactions may occur between the liquid metal and the coating at high temperature, because most metals become very reactive as they become liquid.

Most of the following techniques can be applied to measurements on solids, as well as on liquids, whereas some techniques or apparatus are specially designed just for measurements on solids or liquids. If this applies to a method a separate annotation will be made.

3.2 Steady state techniques

Traditional classification distinguishes four absolute steady state techniques for measuring: *axial heat flow, radial heat flow, guarded hot plate, and direct electrical heating*.

Axial heat flow method

In the axial heat flow method, a known thermal flux q is applied to one end of the sample and removed at the other end by a heat sink.

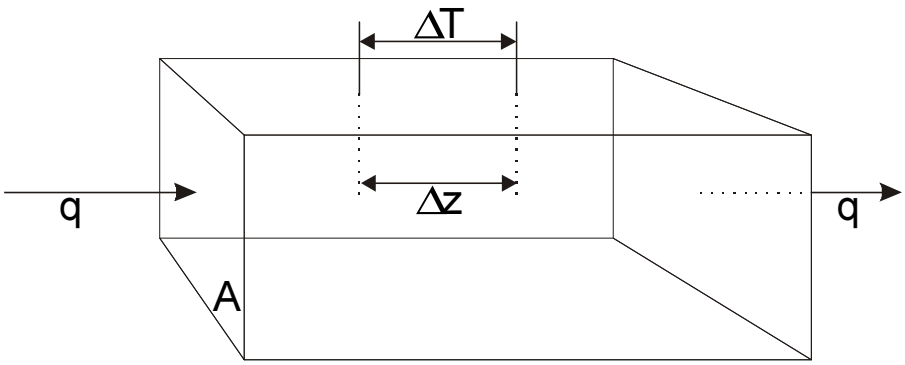

Fig. 2: Schematic representation of the axial heat flow method.

Thermal conductivity can be calculated by the following equation

$$\lambda = \frac{q}{A} \cdot \frac{\Delta z}{\Delta T} \qquad \textbf{2-1}$$

where q is the heat flux traversing through the specimen of cross-sectional area A and $\Delta T/\Delta z$ is the constant temperature gradient along the specimen, usually determined from the temperatures T_2 and T_1 ($\Delta T = T(z_2) - T(z_1)$) of sensors located at z_2 and z_1. The evaluation of λ therefore involves the following:

1.) The determination of the geometrical parameters A and $\Delta z = z_2 - z_1$.
2.) Assurance that the heat flow pattern is indeed unidirectional. This usually involves both, careful design of experimental configurations, and active "temperature matching" of various components of the apparatus during the experiment.
3.) Compliance with the requirements of steady state conditions.

4.) Measurement of q, usually generated in some heater attached to, or embedded in, the specimen. This measurement itself is normally a standard operation, but difficulties are encountered in ensuring that all the measured power (heat flux) is responsible for the measured temperature gradient $\Delta T/\Delta z$.

5.) The measurement of the temperature of the two (or in some methods more) sensors, T_2 and T_1. As with the power measurement, this, by itself, is again straightforward; however, ensuring that the measured sensor temperature corresponds to the specimen temperature at the presumed locations z_2 and z_1, is not trivial.

These five points are common to all "unidirectional" steady state methods, although their relative importance may vary from technique to technique. In general, 1.) and 3.) are straightforward, the other three troublesome. For the axial heat flow technique, 5.) is the most important factor at low temperatures, and 2.) at high temperatures.

This principal problem at high temperatures is related to the prevention of heat losses by convection and radiation; it is usually overcome by using insulation materials and heated guard shields. By using insulation materials or heated guard shields, Eq.(3-1) has to be rearranged:

$$\lambda = \frac{1}{A}\left(\frac{q\Delta z}{\Delta T} - \lambda_c A_c \right) \qquad \textbf{2-2}$$

The subscript c denotes properties of the surrounding cell.

The biggest advantage of the axial heat flow is the simple geometry and the more or less simple setup. This method has been used to determine the thermal conductivity not only of solids but also of various liquid metals with low melting points including Hg, Pb, In and Ga [NPL Report, 1997].

Radial heat flow method

Fourier's law for steady state heat transfer holds regardless whether the temperature gradient is linear or cylindrical.

Fourier's law for 1 dimension reads:

$$q = -\lambda \cdot \frac{dT}{dx} \qquad \textbf{2-3}$$

Fourier's law can be translated to a cylindrical geometry by recognizing that the surface area of a cylinder is $2 \cdot \pi \cdot r \cdot L$. The heat flows from the inner (r_1) to the outer (r_2) radius at temperatures T_1 and T_2 respectively. By rearranging Eq.(3-3) under consideration of these facts, one gets the following:

$$\lambda = \frac{q}{L} \cdot \frac{\ln\left(\frac{r_2}{r_1}\right)}{2\pi(T_1 - T_2)} \qquad \textbf{2-4}$$

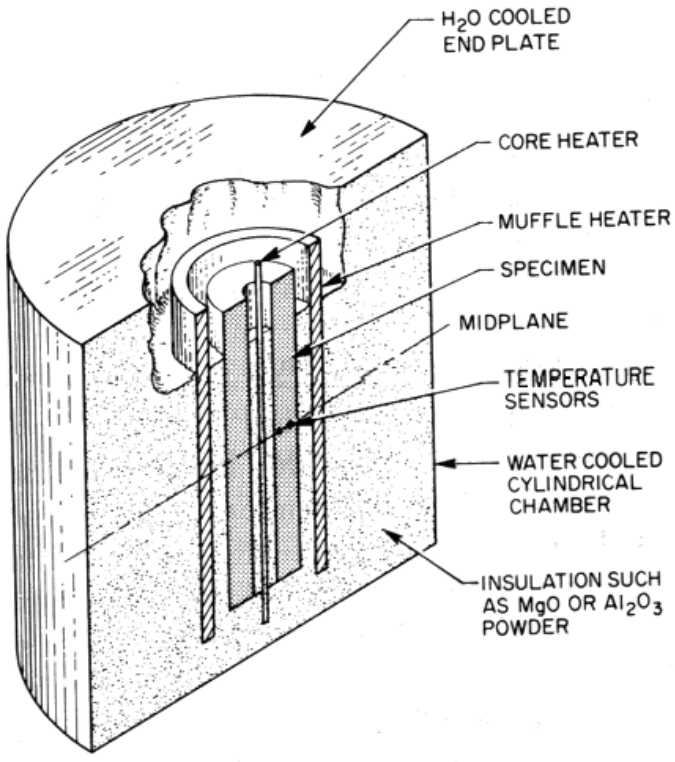

Fig. 3: Schematic of a fundamental radial heat flow apparatus. The temperature sensor positions are denoted by •. [Maglić, 1984]

Fig.(3) shows the schematic of an apparatus used for radial heat flow measurements. The thermal conductivity is calculated by using Eq.(3-4) where q/L is the heat flux per unit length from the core heater over the specimen midplane and T_n is the temperature at radius r_n.

This configuration will yield accurate data if the ratio of specimen length L to diameter d is sufficiently large to ensure that all heat flow at the specimen midplane is radial.

The greatest advantage of a radial heat flow apparatus is its high accuracy at elevated temperatures. A secondary advantage arises from the fact, that these systems can be operated with relatively simple instrumentation. An additional advantage is its applicability on specimens with very high and very low thermal conductivities.
The greatest disadvantage of the radial heat flow technique is the large specimen size, which can lead to undesirable high specimen cost, assembly difficulties, and slow operation.

The radial heat flow method can also be adapted for measurements with molten metals. This method is sometimes called *concentric cylinder method* instead of radial heat flow method.

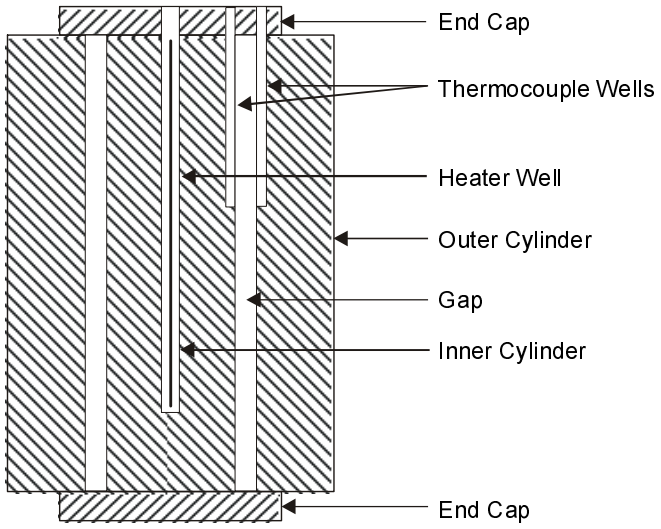

Fig. 4: Schematic diagram of the concentric cylinder method

The adapted apparatus consists of the two concentric cylinders with a gap between them. The molten metal is placed in the annulus between the cylinders and the known heat flux q is supplied to the inner cylinder and the temperature difference ΔT between the two cylinders is monitored.

As one can see, the radial heat flow method is adapted for molten metals by producing a container for the liquid but the rest of the measurement stays exactly the same. Unsurprisingly, as the technique equals the radial heat flow method, the thermal conductivity is also calculated by Eq.(3-4). As a sort of heredity the concentric cylinder method suffers from the same problems - such as assembly difficulties or slow operation - as its origin.

Direct heating method

There is a general class of thermophysical determinations which utilize Joulean heating generated by electrical current flowing through the sample to control the sample temperature gradients during the property measurements. This class is combined as "direct electrical heating methods". They are distinguished by the lack of external furnaces to control the specimen temperature. This in turn greatly shortens the time to attain an equilibrium temperature and easily permits transient measurements. These methods are limited to reasonable electrical conductors but allow the use of different specimen forms such as wires, rods, tubes, or sheets.
The greatest advantage of this method except of the lack of an external furnace is the opportunity to yield more than one property by measuring several properties simultaneously.

The measurements of this work were performed with a direct electric heating setup, but with a dynamic measurement technique instead of the steady state measurement. See the pulse-heating section at the end of this chapter for more specific details on this method.

Guarded hot plate method

The guarded hot plate method is a steady state axial heat flow measurement of thermal conductivity for disk-shaped specimens. The heat flow is measured in a similar way as the radial heat flow and the hot wire technique; thermal dissipation due to Joulean $I^2 \cdot R$ heating of a central heater. This technique is generally regarded to be the most accurate measurement technique in the field of steady state experiments.

There are two different apparatus for this method: The first and more common one is the two-specimen setup, the second one is the single-specimen setup. The experimental configurations for the technique are shown in Figures (5a, 5b):

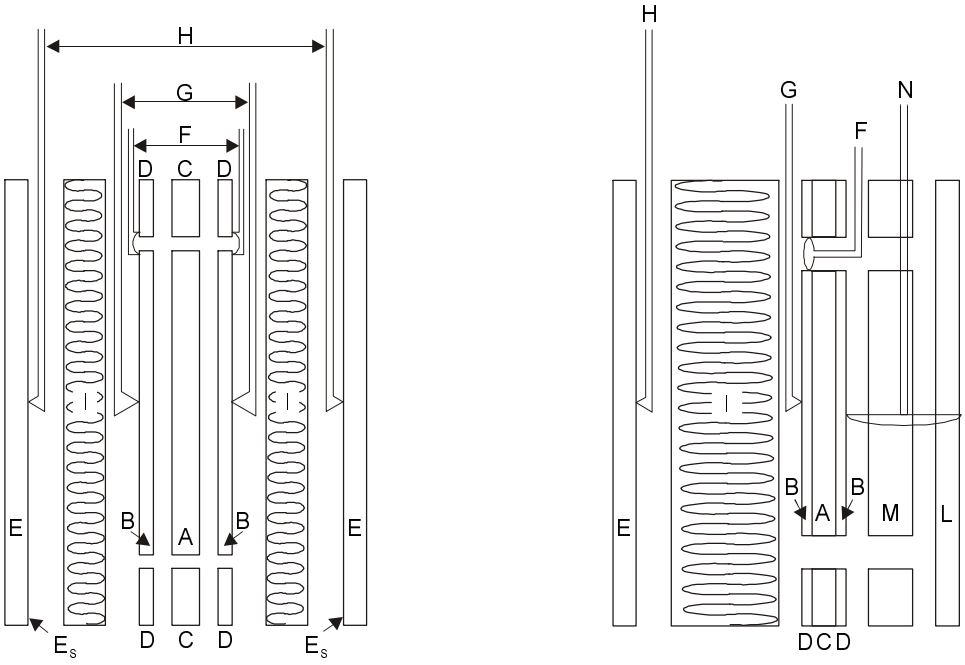

Fig. 5: General features of two-specimen and single-specimen hot plate apparatus.

a) two-specimen apparatus

b) single specimen apparatus

Key: A, metering area, heater; B, metering area surface plates; C, guard heater; D, guard heater surface plates; E, cooling unit; E_s, cooling unit surface plates; F, differential thermocouples; G, heating unit surface thermocouples; H, cooling unit surface thermocouples, I, test specimen; L, guard plate; M, guard plate insulation; N, guard plate differential thermocouples.

In the case of the two specimens method Fig.(5a) the test specimens are symmetrically placed above and below the main heater and the temperature drop across the specimens ΔT is measured by two thermocouples immersed in each specimen, spaced distance L apart. Assuming perfect symmetry in dimensions, thermocouple junction placement, and heat flow through the upper and lower specimen one gets:

$$\lambda = \frac{qL}{2A\Delta T} \qquad \textbf{2-5}$$

In order to guarantee that the heat flow from the metered area is one dimensional, that means it flows strictly through the specimens and not out of the side walls of the main heater and the specimens, several guard heaters and guard plates with insulation are used.

In the case of the single specimen method Fig.(5b) one of the cold plates is removed and the auxiliary heater on that side is heated to match the temperature of the metered area. Since no temperature gradient exists in that direction, heat generated from the metered area flows uniaxially through the single specimen. By losing the multiplicity factor 2 from Eq.(3-5) the thermal conductivity is calculated by:

$$\lambda = \frac{qL}{A\Delta T} \qquad \textbf{2-6}$$

In some publications a similar technique is mentioned to perform measurements on liquid metals called *parallel plate method*. This method is mostly the same as the single specimen guarded hot plate method and uses also Eq.(3-6) to calculate thermal conductivity. The only major difference in the setup are the expansion volumes used to compensate thermal expansions through the measurement process.

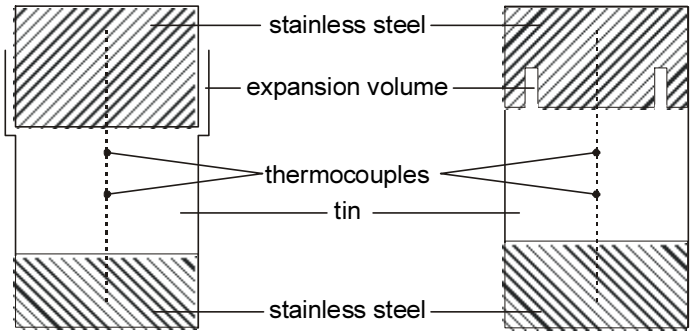

Fig. 6: Schematic diagram of parallel plate apparatus

Calorimeter method

An additional method to the four traditional techniques is the calorimeter method. This is an older technique which is a direct measurement of the Fourier's law. It is one of the ASTM (American Society for Testing and Materials) standard tests for thermal conductivity. The experimental configuration is shown below:

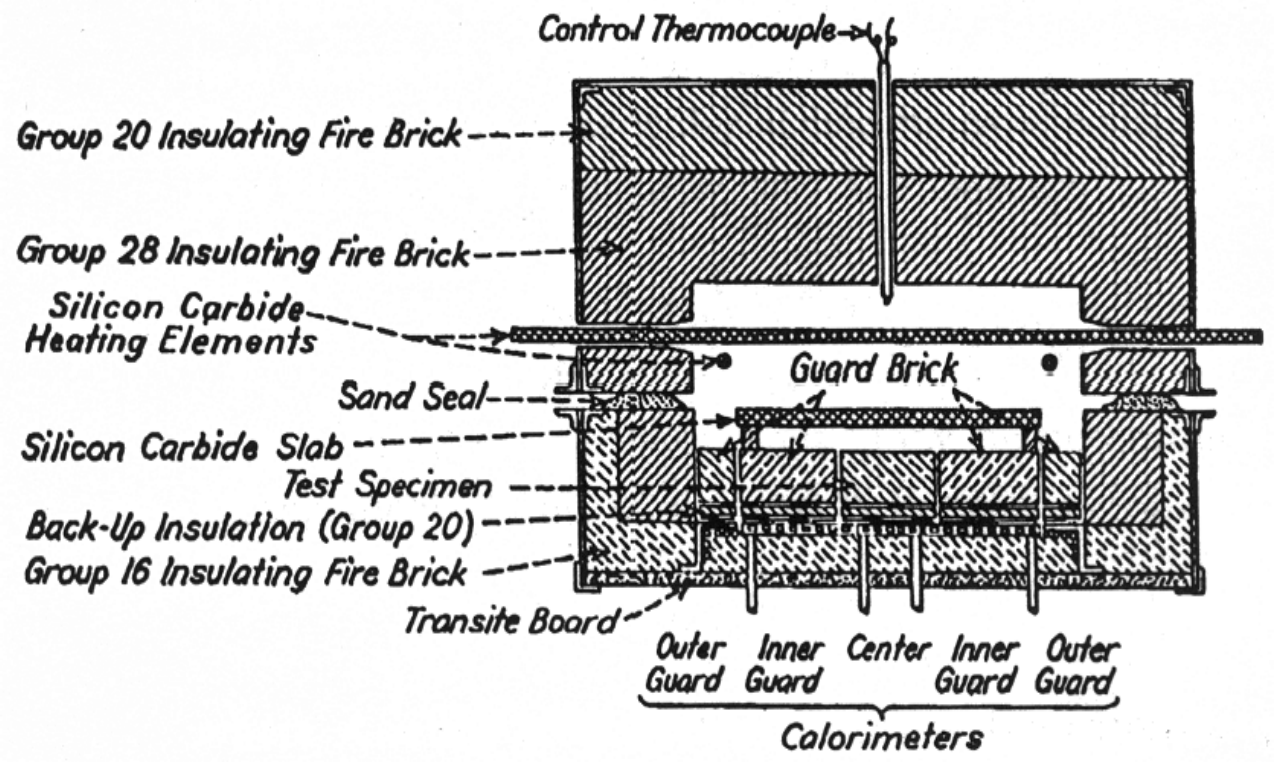

Fig. 7: Schematic of the calorimeter method of measuring thermal conductivity. Specimen sizes are approximately three bricks of dimension 23 x 11,4 x 6,4 cm^3. [Speyer, 1994]

A SiC slab acts to distribute temperature gradients from the heat source (usually SiC or $MoSi_2$ heating elements). The test specimen is bordered by two insulating guard bricks, and these guard bricks as well as the specimen are in thermal contact with a water-cooled Copper base. The Copper base is made up of several separated water cooling systems: A center system is the calorimeter, which is surrounded by the inner and outer guards. The calorimeter has a smaller area than the test brick. The configuration is designed so that there are no temperature gradients in the horizontal planes along the heat flow path to the calorimeter. Thus, the heat flow into the calorimeter is one dimensional.

Two thermocouples separated by distance L are imbedded in the test specimen, one directly above the other, whereby the temperature drop $T_2 - T_1$ between them is measured. A differential thermocouple measures the temperature rise of the exit water of the calorimeter as compared to its entrance temperature. The mass flow rate of water into the calorimeter is monitored, so that over a specific time interval Δt, the total heat absorbed by the calorimeter may be calculated,

knowing the specific heat c_p of water. Dividing by the time interval will give the rate of heat flow into the calorimeter under steady state conditions. Hence, thermal conductivity may be determined by a rearrangement of Fourier's equation:

$$\lambda = \frac{\frac{dq}{dt} L}{A(T_2 - T_1)} \qquad \textbf{2-7}$$

where A is the cross sectional area of the calorimeter, and L the distance between the two embedded thermocouples junctions. Since the heat flow is constant throughout a vertical section of the specimen (steady state conditions), thermocouple junctions measuring T_1 and T_2 can have vertical positions anywhere along the specimen which is one of the advantages of this method.

3.3 Non-steady state techniques

Both methods described in this section are not very common because other measurements (i.e. transient methods) are easier to carry out. Nevertheless, they are included to demonstrate the overall principles of non-steady state techniques, as they are characterizing for this group of techniques.

Radial temperature wave (RTW) technique

In this method the sample is usually cylindrically-shaped and a modulated heat supply is applied along the center of the specimen. The variations in temperature are monitored on the outside of the sample. There is a phase lag between the input and the output and this is related to thermal diffusivity a of the sample. Thermal diffusivities can be derived from the amplitude of temperature oscillations and from the phase differences between them; thermal conductivity is calculated via the WFL and the values calculated with data from this method were found to be in good agreement [NPL Report, 1997].

Plane temperature wave (PTW) technique

This method uses disc-shaped specimens (typically 0,2 mm thick) and plane temperature waves are derived by bombarding the specimen with a harmonically-modulated electron beam and monitoring the phase change of the temperature transient recorded on the other face of the specimen. Measurements can be obtained either at constant temperatures or dynamically with heating rates up to 1000 $K \cdot sec^{-1}$. The results of the two experiments were also found to be in good agreement. For measurements in the liquid phase, only a small portion of the disc is allowed to melt, and readings are obtained for temperatures up to 150 K above the liquidus. Thermal diffusivities for the liquid phase of high-melting metals such as Mo, Ti, Ir, Rh, Pt and Pd were obtained with this method [NPL report, 1997]. It could be argued that convectional contributions would tend to be small due to short duration of experiments in the liquid state, but assumptions may not be valid since circulation flows could arise from buoyancy and thermocapillary forces caused by the large temperature gradients. This method is sometimes referred to as the modulated beam technique.

3.4 Transient techniques

The transient techniques are the historically newest measurement methods. They are easier and faster to carry out than the non-steady state methods and even provide more accuracy.

Transient hot wire method

The hot wire thermal conductivity method involves the placement of a thin refractory wire between two identical refractory plates under investigation. Historically, this is an application of a hot wire method used in the determination of thermal conductivities of liquids and gases.
A constant electrical power is dissipated by the wire as heat into the surrounding refractory, and the temperature of the wire is monitored. If the refractory is highly thermally conducting, the wire temperature will be lower compared to the case when the refractory is highly insulting.

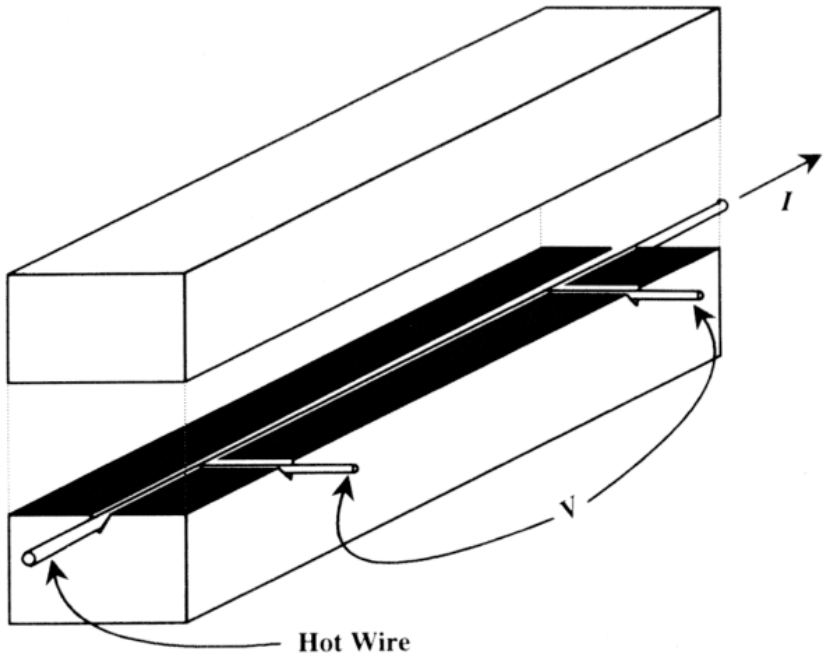

Fig. 8: Schematic of the hot-wire thermal conductivity test. Refractory bricks would be of the same size as in Fig. 7. [Speyer, 1994]

The theoretical model assumes a linear heat source dissipating heat radially into an infinite solid, initially at uniform temperature. The fundamental heat conduction equation in cylindrical coordinates is solved with the initial condition that the temperature of the wire at zero time is T_0 and after some time t, boundary conditions: (1) at infinite radial distance from the wire, the

temperature is still T_0, (2) at a radial position within the refractory, approaching the radius of the wire, steady state radial heat transfer occurs. The solution obtained by LAPLACE transforms is:

$$\Delta T(r,t) = \frac{q}{4\pi\lambda} \cdot \ln\left(\frac{4at}{r^2 \exp\gamma}\right) \qquad \textbf{2-8}$$

Thermal conductivity is given by this equation (3-8), where q is the heat input per unit length of wire, r is the radius of the wire, a is the thermal diffusivity of the material under investigation, γ is EULER's constant ($\gamma = 0.577216$, [Bronstein, 1991]) and t is time. The temperature of the wire is assumed to be constant throughout its volume. Based on this expression, a plot of $\Delta T(r, t)$ versus *ln* time should be a linear increasing function, where the thermal conductivity of the refractory can be directly calculated from the slope, if q is known. (Note that Eq.(3-8) only applies, when $r^2/4at << 1$.)

In practice, only a portion of the *ln* time/temperature plot is linear. A non-linear portion at the start of the curve is a result of steady state conditions not immediately being met at the wire surface. And the non-linear portion after longer times results from the refractory block not actual being of infinite dimensions.
Thermal conductivity measurements are taken at a series of isothermal temperatures, created by an external furnace. The furnace must provide enough stability so that there are negligible temperature gradients within the refractory blocks.

Temperature is measured via a thermocouple junction welded to the center of the hot wire. The legs of the thermocouples extend perpendicular in either direction to the hot wire, and grooves must be cut in the refractory for these wires. A disadvantage of this technique is, that the thermocouple wires may act as heat sinks for the hot wire, which can be avoided or minimized by using thermocouple wire of minimal diameter and a junction bead as small as possible.

In another commonly used configuration of the hot wire method the wire acts both, as a heating element and a resistance thermometer. This special configuration expands the basic method and allows to measure molten metals and liquids with it. Eq.(3-8) holds for all different types of hot wire configurations and the determination of the thermal conductivity via the slope of the ΔT versus *ln* time plot stays the same, too. See Figure 9 for a schematic diagram of this setup.

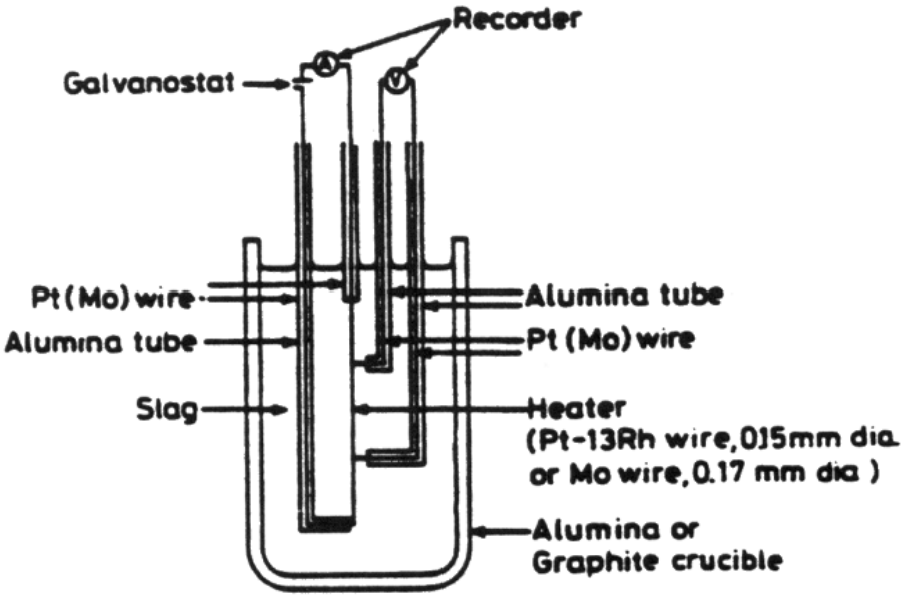

Fig. 9: Schematic diagram showing the transient hot wire method for liquids

When this method is applied to electrically conducting melts it is necessary to apply a coating to the wire to prevent electrical leakage into the melt. Various insulation techniques have been employed, such as:

- using a glass capillary containing liquid Hg or Ga
- application of Al_2O_3 or other insulating oxide layers
- the oxidation of the metal wire to provide a protective coating

However, the application of this configuration may be restricted to temperatures up to 1000 K since with increasing temperatures the coatings become progressively (i) more conducting, (ii) more vulnerable to chemical attack, and (iii) the mismatch in thermal expansion of metal and coating become more pronounced and can lead to spalling.

Laser flash (or pulse) method

The laser flash method differs from the other methods discussed above in this chapter in so far as it is a method of measuring the thermal diffusivity instead of the thermal conductivity. The thermal conductivity may be obtained from the thermal diffusivity if the specific heat and the

density of the material under investigation are known. (See the Chapter 4: Experimental setup and data evaluation for more details.)

The flash method entails a short pulse of high intensity energy, absorbed by the front surface of a small specimen shaped in the form of a disk. The radiant energy source can be a xenon flash lamp, an electron beam, or - most common - a laser. The energy propagates due to conduction and, at higher temperatures, radiation toward the back surface of the specimen. By monitoring the temperature rise of the back face of the sample thermal diffusivity can be obtained.
A number of simplifying assumptions are needed for a mathematical model for this method like: The flash is uniformly distributed across the front face and absorbed within a thin layer relative to its overall thickness, or the heat propagates one dimensionally toward the back face, etc.. The whole mathematical model is explained in different publications e.g. [R.F. Speyer, Thermal analysis of materials, 1994].
During the derivation one obtains the later on used result that the temperature transient at the back face exhibits a maximum ΔT_{max} as a consequence of radiation losses. Assuming that the assumptions of the model have been met experimentally, by determining the time $t_{1/2}$ corresponding to the temperature at half maximum $\Delta T_{max}/2$, thermal diffusivity can be calculated by:

$$a = \frac{0.1388 \cdot l^2}{t_{1/2}} \qquad \textbf{2-9}$$

where a is the thermal diffusivity and l the thickness of the sample.

In practice, other fractions t_γ can also be used, but a different constant must be employed. These constants are tabulated for different fractions.

This method has been widely used for measurements on solids. For the use on liquids, it must be modified since it is necessary (i) to contain the sample and (ii) to mount the disc horizontally.

A laser is used to supply the heat pulse and the temperature of the back face is monitored by an infrared detector (i.e. InSb). The sample is contained in silica or sapphire cells which are transparent to infra-red radiation. The thickness of the specimen must be carefully selected with regard to the thermal conductivity of the sample. Carbon is frequently applied to the surface of

the metal to improve the absorption of the energy pulse. It is difficult to maintain disc shaped geometry for liquid metals which are non-wetting on sapphire (or silica) and consequently reliable measurements can not be obtained for these conditions. Corrections are usually applied to account for expansions of the metal.

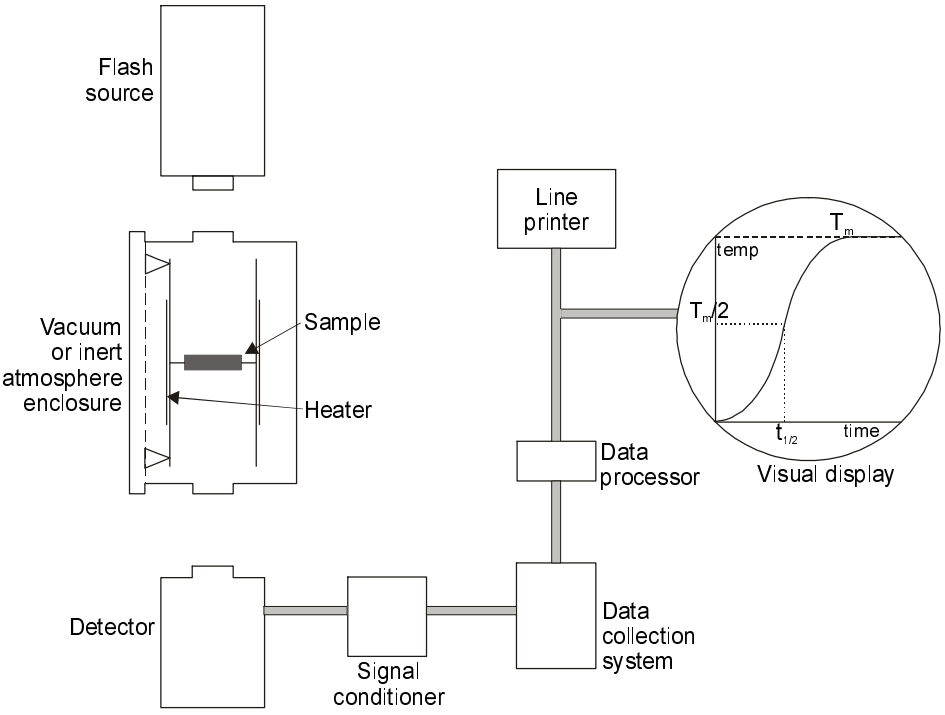

Fig. 10: Schematic diagram illustrating (i) typical laser pulse apparatus used to determine thermal diffusivity of liquid metals and (ii) typical transient display.

The principle advantages of this technique are:

- it is robust and involves no contact between the probe and the melt
- the method is well-proven and widely used on solids

Possible disadvantages of the method are:

- transient times in liquid metals are up to 2-3 seconds and some convectional flows may be initiated which could affect the results
- reactions between the liquid metal and the container may also affect the results
- the application of carbon to improve energy absorption is not desirable for metals such as *Fe* which have appreciable carbon solubility

3.5 Pulse-heating techniques

Classification

The pulse-heating method is now going to be discussed, the technique the measurements of this work were made with. There are two different reasons why this method was not handled earlier in the survey: (i) it's the method whose theory and experimental details are best known within our workgroup, (ii) somehow pulse-heating does not fit in any of the 3 categories dealt within this chapter.

The classification of the pulse-heating method is a little bit difficult and confusing: on one side it does not apply to the transient techniques, because temperature gradients are of the order of some 10^2 K and on the other side it can't be a non-steady state technique because of the short time regime of about 10^{-8} to 10^{-6} sec. To handle this "unclearness", we decided to explain pulse-heating as a stand-alone technique.

Principal considerations

As mentioned before, the principle method of Joulean $I^2 \cdot R$ heating generated by an electrical current flowing through a sample is not restricted to steady state techniques; on the contrary, it's widely used in dynamic measurements because of the ability to reach temperature regions which are impossible to get to with steady state methods. Traditional steady state techniques are generally limited to temperatures up to about 2500 K. This limitation results from different reasons:

- chemical interactions of the specimens with its containers
- the loss of mechanical strength
- increasingly more problems with heat transfer, evaporation and electrical insulation as temperature rises while the samples and its environment are kept for times up to hours at high temperatures

As a way out fast dynamic methods such as pulse heating have been developed to avoid these difficulties and permit the extension of the experimental range some 10^2 K into the liquid phase.

Experimental details

Rapid volume heating methods involve resistive self-heating of the specimen by passing an electrical current pulse through it. Starting at room temperature, measurements can be performed far into the liquid phase of the material under investigation. Depending on the heating rate required, the electrical energy is stored in a battery-bank (slow) or in a capacitor-bank (fast). Measurements can be performed either in an air-, or an inert-gas atmosphere.

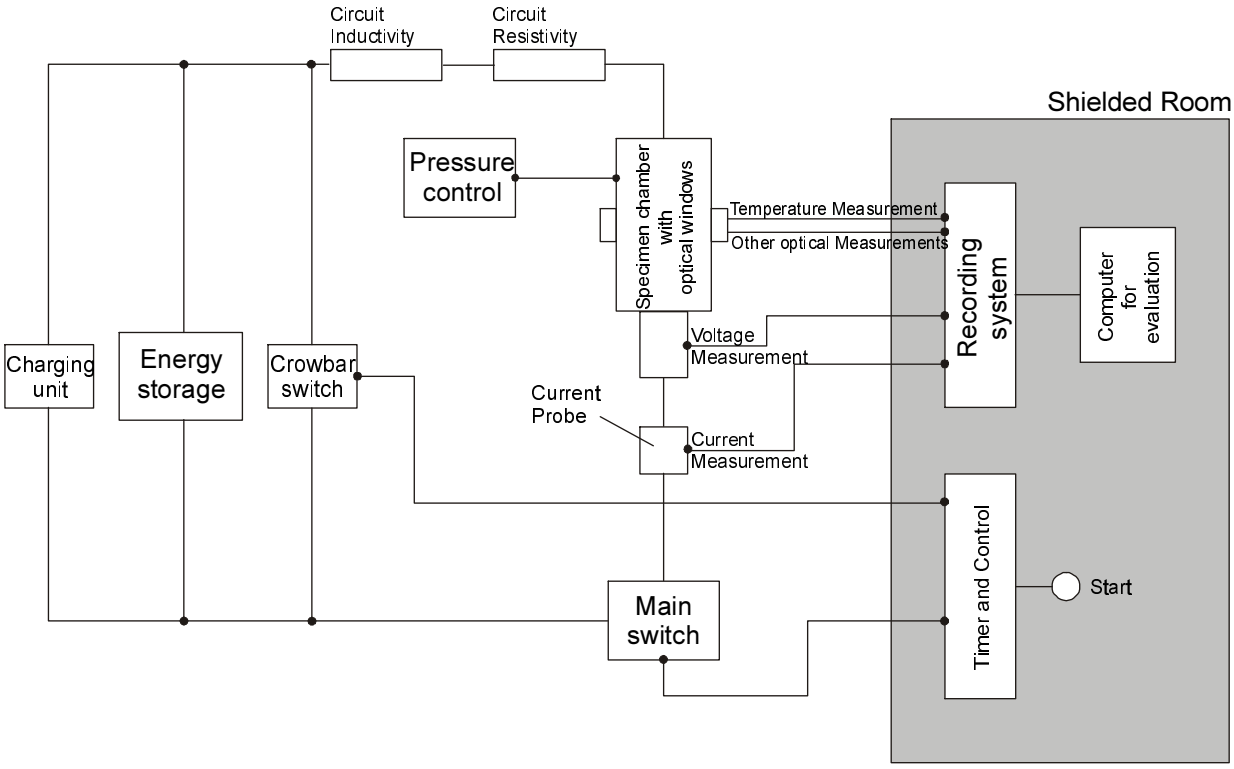

Fig. 11: Schematic display of a standard resistive pulse-heating system

Figure (11) shows a functional diagram of a typical pulse-heating system which should help to explain the major parts for such a measurement. The details of the components vary with the time scale of the measurement.

The discharge circuit consists of the energy storage, the main switch (i.e. high voltage mercury vapor ignitron tube), and of the specimen chamber with windows for optical diagnostics. An additional requirement is the crowbar switch to stop the experiment at any desired moment.
The measured quantities are the current through the sample, the voltage drop across the sample, the temperature of the sample which is detected by using optical pyrometers and other optical

measuring instruments such as a camera-system with a CCD-array to determine volume expansion of the sample during the experiment.
Due to the heating rates used, very fast and reliable data acquisition equipment is a must. All of this equipment has to be placed in a shielded room (a so-called "FARADAY-cage").

Pulse-heating methods have been used to measure thermal conductivity, electrical resistivity, specific heat, hemispherical total emissivity, normal spectral emissivity, thermal expansion, and properties derived from the primary properties such as enthalpy, thermal diffusivity, coefficient of linear expansion, and WFL ratio.

Pros and contras of the pulse-heating method

The greatest advantage of pulse-heating (and of course of all direct heating techniques) is surely the fact, that this technique yields more than one property determined at once and, in fact, all the properties listed above can be measured simultaneously (or consecutively with steady state direct heating methods) on the same specimen. Another advantage is, that samples can be used in a lot of different forms such as rods, tubes, plates, and wires.

On the contrary, the greatest disadvantage is the fact that this method is limited to electrically conducting materials. A second disadvantage is the extensive experimental setup needed for measurements in the µs-time regime.

Chapter 3

Experimental setup and data evaluation

4.1 Experimental details of the pulse-heating setup

As mentioned in the last chapter, the measurements of this work are performed with a resistive pulse-heating apparatus, our so called "slow discharge circuit". The word "slow" refers to the time regime - 50 to 100 μs - covered by our measurements. (We also have a "fast" discharge circuit, which means a duration for one measurement of about 2 to 4 μs.) The principle of this apparatus is more or less the same as shown in Fig.(11) but differs in experimental details like the optical detection, or the voltage measurement. For better understanding, take a look at Fig.(12) at the end of this section, which shows a schematic diagram of the discharge circuit used in our laboratory.

During a measurement, very high currents (about 10^4 A) can occur, depending on the specimen and the charging voltage. Due to this fact, very appropriate electrical shielding is needed for all the instruments, leads, and detectors. All electrical leads are provided with coaxial cables and shielded within Copper tubes to minimize electrical interference on the signals. (The amplifier electronic is shielded twice to prevent interference.) The large-scale shielding pays off, as we can reach heating rates up to 10^8 K/s. The energy storage fitted into the circuit is a 550 μF capacitor bank which could be charged up to about 10 kV using an high voltage power supply.

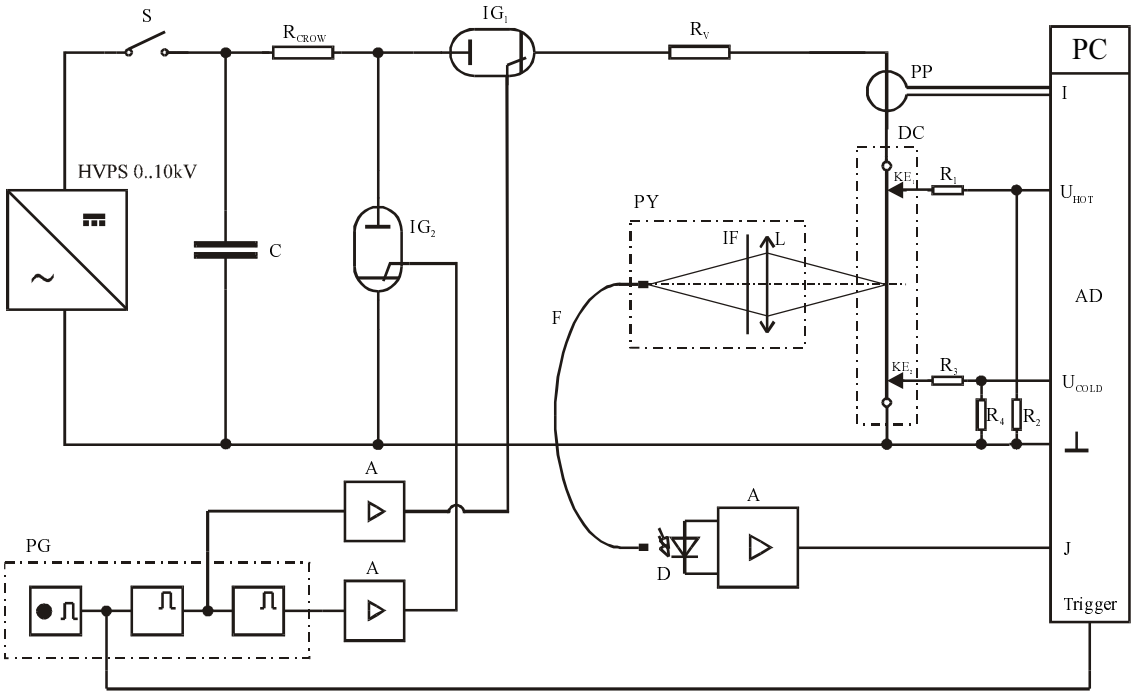

Fig. 12: Schematic diagram of the discharge circuit in Graz

Key: HVPS, high voltage power supply; C, capacitor bank; S, switch; R_{crow}, crowbar resistor; R_v, variable resistor; $IG_{1,2}$, ignitrons; PG, pulse generator; A, amplifier; PP, Pearson probe; DC, discharge chamber; $KE_{1,2}$, knife-edges; R_1-R_4, ohmic voltage divider resistors; PY, pyrometer; L, lens; IF, interference filter; F, light-fiber; D, photodiode;

4.2 Measured and calculated properties

Our pulse-heating apparatus enables us to measure 4 different time resoluted quantities simultaneously during one single experiment. Additionally we can make supplementary optical measurements like stability investigations on the wire without affecting the principle measurement. These 4 quantities we basically measure are:

- the current through the wire
- the voltage drop along the wire
- the radiance of the wire surface
- the volume expansion of the wire

As the newest addition to our experimental setup, we got a Division of Amplitude Laser Polarimeter (DOAP), which allows us to measure the emissivity ε (at λ = 684 nm) time resolved

and simultaneously with all the other signals. Up to now, the emissivity measurement is still in its test phase and has not become one of our standard properties to measure. First results are very encouraging and hopefully we can add the emissivity to the list of constantly determined properties during the next year.

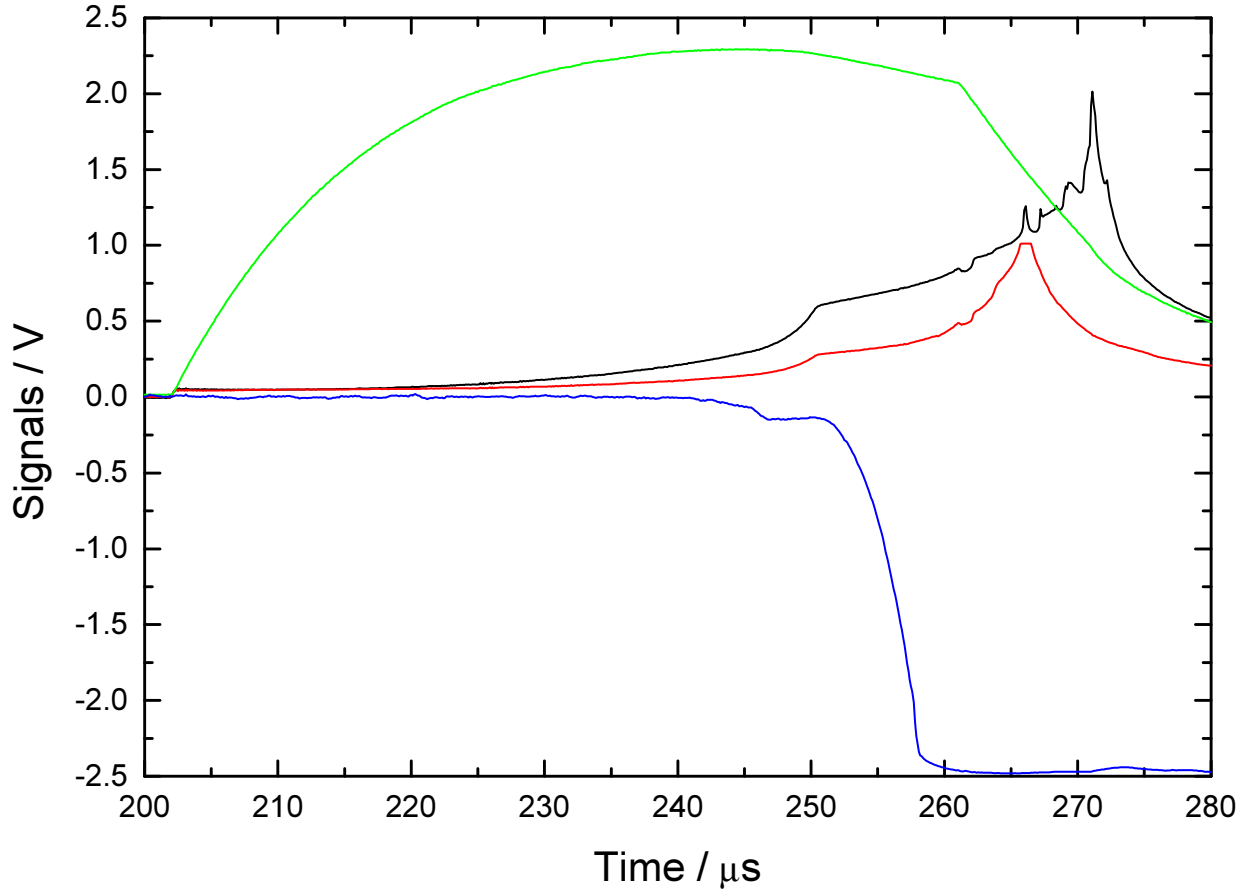

Fig. 13: Plot of the electrical raw-signals detected during one experiment. Signals: green: current, red, black: voltages, blue: surface radiance. The nearly horizontal line in the radiance signal between 246 and 250 µs is the so called melting-plateau, the solid-liquid transition of the wire. Crowbar at 261 µs. (Note: For ease of graphical representation, the radiance signal of the pyrometer has been divided by a factor 2.)

Starting with these four quantities we obtain most of the desired thermophysical properties by simple calculations. A survey of the properties we are able to determine is given in the following paragraphs:

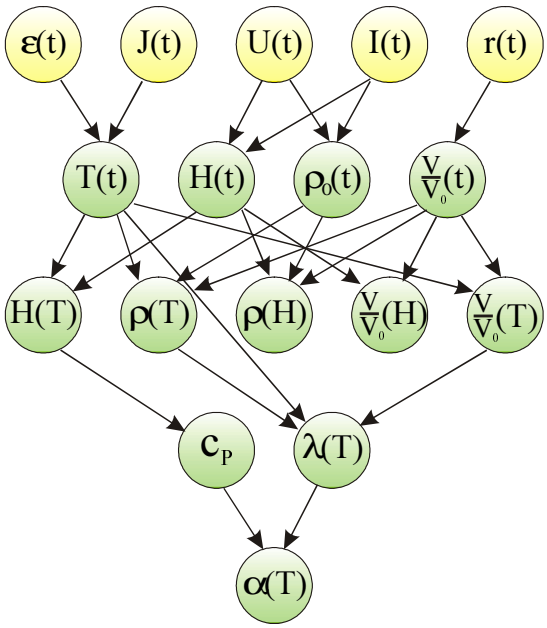

Fig. 14: Schematic diagram of the measured quantities and the properties calculated from the original signals. Quantities in yellow circles are the measured ones, green circles are indicating the derived properties. (Note: in this graphic the emissivity ε appears as a fifth measured property although we do not measure it permanently yet. It is part of the current project we are running right at the moment.)

The following section displays in short terms the measurement of each of the four properties and the relations used to calculate all other properties from the measured ones.

4.3 Data evaluation

The current

A resistor R_v (0,5 to 1,5 Ω) is used to realize a resonant circuit to shape the current pulse as rectangular as possible. (See current signal in Fig.(13).) The discharge is promptly started and aborted by two ignitrons, which are very fast switches. The first one starts the measurement, whereas the second ignitron crowbars the discharge with another resistor R_{crow}.

The current in the discharge circuit and through the wire is measured via a Pearson probe (Pearson Electronics, type 3025) using the induction principle. To get a current signal which is direct proportional to the voltage through the probe a RC-component is integrated in the probe. The calibration factor for the probe is 79,6 A/V.

All electrical signals recorded with the data acquisition equipment have to be in the range of ± 5 volts, not to overload the data acquisition cards in the computer, which is guaranteed by using calibrated ohmic voltage-dividers.

The voltage divider factor for the current has been determined as:

Divider-Ratio: 1 / 60,3 ± 0,1

The voltage

Actually, it's not the voltage we measure, but the voltage drop between two knife-edge probes and ground. These knife-edge probes are 0,1 mm Tantalum strips, which are v-shaped on one end. The knife-edge probes are placed at both sides of the wire with the specimen running through the v-shaped cutting. The distance between the two probes has to be measured with a travelling microscope, because this actual length is used for the calculation of the specific conductivity.
The desired result is the voltage drop across the wire, which is obtained by subtracting the two voltage signals. This method helps us to cancel out the arbitrary resistance at the contact points of the knife-edge probes with the wire, which would be nearly impossible to determine.

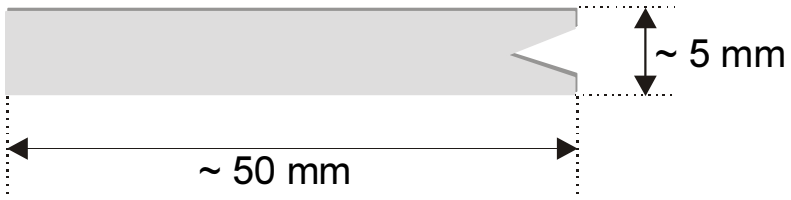

Fig. 15: Schematic drawing of the knife-edge probes. (One of the probes can be seen in Fig. 16a)

As with the current signal, both voltage signals have to pass through voltage-dividers to guarantee that they are in the range of our measurement electronic (see the paragraph handling the current-signal above). The factors for the dividers have been calibrated to:

Divider-Ratio$_{hot}$: 1 / 1029,4 ± 0,4

Divider-Ratio$_{cold}$: 1 / 309,4 ± 0,2

The subscript hot marks the voltage signal next to the current injection, the subscript cold the voltage signal on the other side of the wire.

The measured voltage signal consists of the following three terms and has to be treated a little bit to get the desired result:

$$U(t) = I(t) \cdot R_s(t) + (L_s + L_c) \cdot \frac{dI(t)}{dt} + I(t) \cdot \frac{dL_s(t)}{dt}$$

3-1

where U(t) is the measured voltage signal, I(t) is the current, R_s is the resistivity of the sample, L_s is the inductance of the sample, and L_c is the inductance of the cell.

The first term in Eq.(4-1) is the desired voltage drop across the wire. The second term represents the inductive component of the voltage signal, caused by the inductance of the circuit and the sample while being treated with a changing current pulse. This term has to be compensated, which is done with a computer evaluation program by approximating the actual course of the signal with a polynomial fit and subtracting the two curves. (For further details see [Sachsenhofer, 2000].) The third term takes the change of wire-inductance into consideration, which is caused by the volume expansion of the sample. This term is only a small contribution to the total voltage signal and can be neglected without affecting the result at all. (See Chapter 6: Estimation of uncertainty for more details.)

The surface radiance

The only way to measure temperatures in a range from 1000 to some 10^3 K is by using an optical pyrometer. Not only is the pyrometer the only reliabel method of measuring high temperatures, but it also has all the advantages of an optical method: it's fast enough to follow rapid temperature changes, it does not need direct contact with the specimen, and does not affect the electrical measurements.

The principle of the pyrometer used can be explained as follows: The light (visible as well as infrared) emitted from the heated surface passes through an interference filter (to select a specific wavelength) and a lens collects the light and projects an image of the wire on the entrance slit of a light-fiber. Through this fiber the light is transported to the pyrometer circuitry, where it's

detected by an InGaAs-photodiode and the voltage signal is amplified with an op-amp. This amplified signal is detected and recorded with a computer.

Table 2: Specifications of the interference filter used for the measurements on Copper

Filter type	Center wavelength [nm]	Bandwidth [nm]	Blocking [nm]
bandpass	1570	84	UV to 3500

In Fig.(13) the nearly horizontal area between 246 and 250 µs in the surface radiance signal indicates the melting of the wire, where the temperature stays more or less constant unless the entire specimen is molten.

The volume expansion

The wire is illuminated by a flash-lamp and the picture is projected via a lens on a multi channel plate (MCP). A special technique of shifting the exposed area on the CCD array enables us to take every 10 µs a picture of the expanding wire from which we determine the volume expansion during the experiment.

These present measurements on Copper have been performed without the expansion measurement, because of the following reasons: (i) the CCD-camera was at the manufacturer for repair and improvement, (ii) the CCD-array read-out process of our second camera is too slow for accurate measurements (only one picture per 500 µs possible), (iii) several investigators have studied the volume expansion during heating of pure Copper, so that the results are well known and found to be correct. Since every measurement contains systematic errors and uncertainties, which are difficult to estimate, we decided to use the recommended values from well known sources (e.g. [Touloukian, 1967] or [NIST, 1990]), which are very accurate and well proven, instead of measuring the volume expansion ourselves at all costs.

The temperature

The temperature is calculated by using an adapted version of PLANCK's law of black body radiation:

$$T = \frac{c_2}{\lambda \cdot \ln\left\{1 + \frac{\varepsilon(T)}{\varepsilon(T_m)} \cdot \frac{J_m(T_m)}{J(T)} \cdot \left[\exp\left(\frac{c_2}{\lambda \cdot T_m}\right) - 1\right]\right\}}$$

3-2

where c_2 is PLANCK's second constant ($c_2 = 1{,}43879 \cdot 10^{-2}$ mK [Bergmann-Schaefer, 1990]), λ is the wavelength selected by the interference filter (λ = 1570 nm), ε is the emissivity; J is the radiance intensity detected by the pyrometer; the subscript m denotes the temperature at the melting point.

Since the emissivity $\varepsilon(T)$ of most liquid metals is unknown, an assumption has to be made for the ratio $\varepsilon(t)/\varepsilon(T_m)$ in the liquid phase of the metal. $\varepsilon(T_m)$ is the value of the emissivity of the sample at the melting temperature T_m, where temperatures are calculated by forming ratios of radiance J(T) at a temperature T to the radiance $J_m(T_m)$ at T_m. The melting temperature T_m is taken from literature data.
Up to now a constant emissivity $\varepsilon(t)/\varepsilon(T_m) = 1$ was assumed for the liquid phase for pulse-heating experiments. Simulations showed [Seifter, 1996], that a change of emissivity during the liquid phase does not affect the temperature results too much.

At the moment we are forcing emissivity measurements with our laser polarimetry apparatus. With this system we are able to determine the absolute value of emissivity ε of the specimen at melting and throughout the liquid phase on one wavelength at 684 nm.

The enthalpy

With the detected electrical signals voltage and current it is possible to determine the enthalpy induced into the wire by Joulean heating. The enthalpy is calculated with:

$$H(t) - H_{298K} = \frac{1}{m} \cdot \int_0^t I(t) \cdot U(t) \cdot dt$$

3-3

where H_{298K} is the enthalpy at room temperature and is commonly set to the arbitrary value $H_{298K} = 0$ and can hence be omitted; m is the mass of the wire determined from the density of the metal and the length of the wire (length measurement of the wire between the two knife-edge probes).

The enthalpy determination is one of the biggest advantages of the pulse-heating method, because the enthalpy by Joulean pulse-heating experiments equals the energy absorbed by the wire. Therefore, we can calculate directly the absorbed energy of the wire at any given time.

The specific heat

As we have seen, Eq.(4-3) allows to calculate enthalpy H of the wire by measuring the current and the voltage across the sample. But there is another relation that holds for the enthalpy:

$$H(T) = \int_{298K}^{T} c_p(T) \cdot dT$$

3-4

where c_P is the specific heat of the specimen under constant pressure.

Rearranging leads to:

$$c_P(T) = \frac{\partial H(T)}{\partial T}$$

3-5

By taking a closer look at Eq.(4-5) one can see, that the specific heat can be determined from the slope of the linear sections of the curve enthalpy H versus temperature T.

The electrical resistivity

The uncorrected electrical resistivity ρ_o (no actual volume expansion considered) can again be calculated from our originally measured properties current and voltage, by using the following relation:

$$\rho_0(t) = \frac{U(t)}{I(t)} \cdot \frac{r_0^2 \cdot \pi}{l}$$

3-6

where r_o is the radius of the wire at room temperature, and *l* its length.

Since the radius of the wire changes during the experiment (because of the volume expansion) it could not be regarded as constant. If we neglect the radial expansion, we get the uncorrected electrical resistivity. Consequently, by considering the radial expansion one gets the corrected electrical resistivity with:

$$\rho_{corr}(t) = \rho_0(t) \cdot \frac{r^2(t)}{r_0^2} \qquad \textbf{3-7}$$

where $r^2(t)/r_0^2$ is the radial (or volume) expansion of the wire.

For further calculations the electrical conductivity σ is needed which is clearly connected with the electrical resistivity trough the elementary relation:

$$\sigma = \frac{1}{\rho_{corr}} \qquad \textbf{3-8}$$

The thermal conductivity

As already shown in Chapter 2.2.2, electrical conductivity and thermal conductivity are tied together through the WIEDEMANN-FRANZ-LORENTZ (WFL) law:

$$\lambda = \frac{L \cdot T}{\rho_{corr}}$$

3-9

The published values for the LORENTZ-number at the melting temperature differ in the range between 2,25 - $2{,}60 \cdot 10^{-8}$ V^2/K^2 for different metals. Although we most commonly use the value $2{,}45 \cdot 10^{-8}$ V^2/K^2 [Weißmantel and Hamann, 1980] for the LORENTZ-number, we decided to use another, higher value in this work on the basis of the work of [Tye, Hayden, 1979]. They

determined LORENTZ-numbers for Copper at different temperatures which are consequently > $2{,}45 \cdot 10^{-8}$ V^2/K^2. As these values change for different temperatures, we assume that the value for the LORENTZ-number for Copper is in the investigated temperature range from 1100 K to 2000 K:

$$\mathbf{L = 2{,}50 \cdot 10^{-8}\ V^2/K^2}$$

The thermal diffusivity

The equation for determination of thermal diffusivity *a* has already been mentioned before in Chapter 2.1. By proceeding from the thermal conductivity λ, the specific heat c_P and the density d of the wire, one gets:

$$a = \frac{\lambda}{c_P \cdot d} \qquad \textbf{3-10}$$

The determination of T(t), H(t), $\rho_o(t)$, H(T), and $\rho_o(T)$ is carried out with a new data evaluation software programmed by [Sachsenhofer, 2000] as a part of his forthcoming diploma thesis. All other calculations are done by using commercial calculation software such as Origin or Excel.

4.4 Additional measurements

Stability of the wire during the heating process

The stability of the wire during the heating process is one of the most important things while using this sort of pulse-heating technique. The wire has to be heated so fast, that gravity cannot effect the geometry of the wire as a result of inertia of mass. In other words, the wire maintains his initial radial geometry throughout the entire time of measurement which is about 50 to 80 µs. This behavior has to proven by short-time pictures, monitoring the whole wire sample.

There are two different complexes of problems that might occur if the wire is unstable:

- the surface radiance measurement
- the volume expansion measurements

The first point one has to consider is the measurement of the surface radiation. As said before, the radiation emitted by the hot wire is measured with an optical pyrometer. This pyrometer has

to be adjusted in such a way, that the surface of the wire is in the focal plane of the pyrometer lens. Otherwise, the measurements would be not intercomparable. Therefore a more or less perfect optical adjustment is the only way to make corresponding measurements. If - for any reason - the wire moves during the measurement, which means it moves out of the focus of the lens, the pyrometer detects useless and arbitrary radiation intensities.
The second is the determination of the volume expansion. Our CCD-camera for detecting the volume expansion can only take 2-dimensional pictures of the wire. Therefore we cannot directly measure the volume expansion, but only the radial expansion of the wire. Furthermore, we have to assume that the wire maintains its radial geometry to calculate the volume expansion with help of the radial expansion. This means - in other words - that the specimen should not be given enough time for linear expansion during the heating process. So if the wire moves, the radial geometry is no longer guaranteed and all calculated properties cannot be expected to be correct.

Instabilities are mainly caused by:

(i) insufficient charging-voltage; the sample is heated too slow and gets enough time for linear expansion

(ii) irregularities of the sample-geometry (if the samples' diameter is not constant throughout the length; thinner sections are heated faster)

(iii) discharges between the wire and the holding-device

The following section should shortly describe how we avoid all of the beforementioned instabilities, which would cause unwanted troubles. It has to be said generally, that not all materials equally tend towards instability effects. Niobium is one of the more harmless sample materials relating to instabilities. Copper, on the other hand, is very difficult to handle because of its low melting-point and its good electrical conductivity.
The very low resistivity of Copper is the main reason for the difficulties while pulse-heating this metal, since the electrical power absorbed by the sample is direct proportional to the square of the current and to the resistivity ($P = I^2 \cdot R$). Therefore we had to use very high charging-voltages of about 7 - 7,5 kV for our experiments to avoid those instabilities. These high voltages lead to current pulses across the wire and the discharge chamber in the range of 10 kA. Consequently,

these high current pulses heavily support the production of discharges and flashovers (see section for (iii) below).

The only thing we can do concerning (ii) is to treat the wire as carefully as possible. Since we have to purchase the wire and it is coiled up on a spindle we have to stretch it slightly before using it. Another important thing is not to bend the wire while building it into the discharge chamber. It is recommended not to touch the wire with bare hands. Also, we recommend to clean the surface of the wire with Acetone, which leads to better signals because of a cleaner surface.

At least, we have to handle (iii) the glow-discharges and the flashovers between the wire and the holding devices. There is not much we can do about it, except sand the holding devices (made of bronze) with high grade paper to remove depositions from preceding experiments and to make the surface as smooth as possible. (Edges and spikes are the primary source of flashovers)

Once you got used to all of this, it is not that difficult to maintain the stability of the wire although it demands a little bit of patience to handle all of the above.

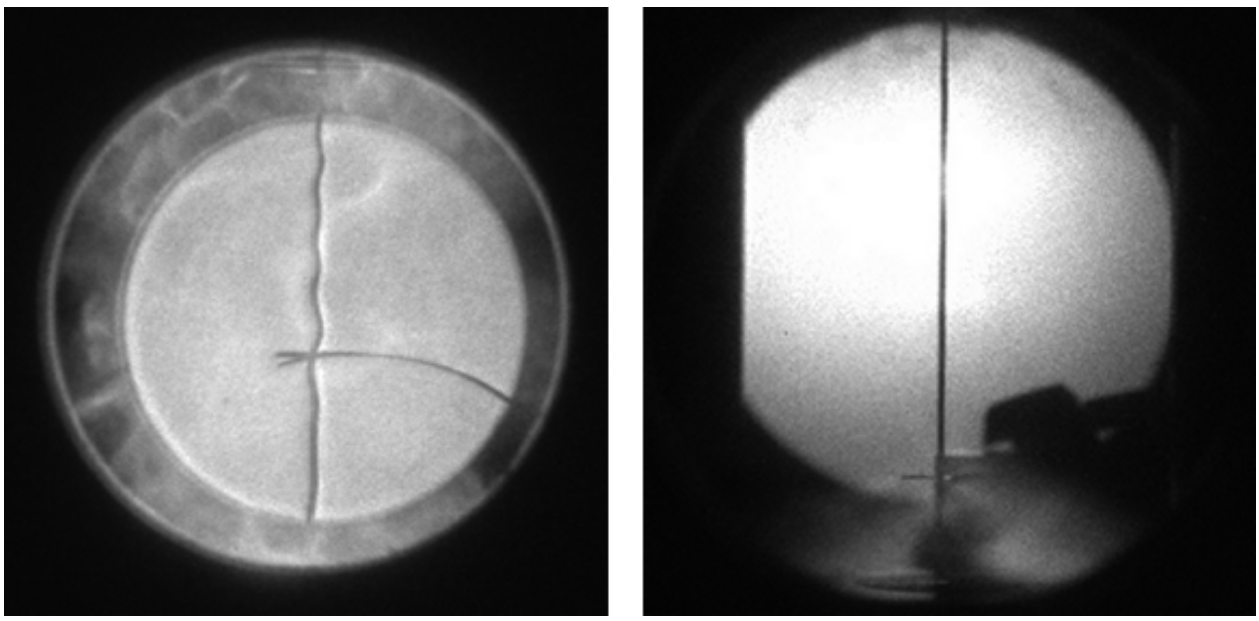

a b

Fig. 16: a) Copper wire with massive instabilities during the heating, b) stable, liquid Copper wire after 252 µs at about 1600 K. Note: the narrow section of the wire in the upper half of 16 b) is not an

irregularity of the wire but an overexposed area at the CCD-array due to the intensity of the background flash

Emissivity measurement

As mentioned before at the beginning of this chapter, we have got a laser polarimetry system to measure the change of emissivity ε time resolved during the entire pulse-heating experiment. The next paragraph deals with this measurement to provide an idea of the technique and the results. For further information about laser polarimetry and the DOAP system, see e.g. [Sachsenhofer, 2000].

The DOAP consists more or less of the following components: a modulated (8 MHz) laser-diode, a polarizer, five detectors (using Lock-In technology), a separated data acquisition, a computer with the data evaluation program and light-fibers for signal transportation. All parts are separately build into the standard pulse-heating setup, not to affect the original experiment.

We performed some experiment with the DOAP on Copper to see if we get practicable results. See Fig.(17) for a typical signal of the experiment:

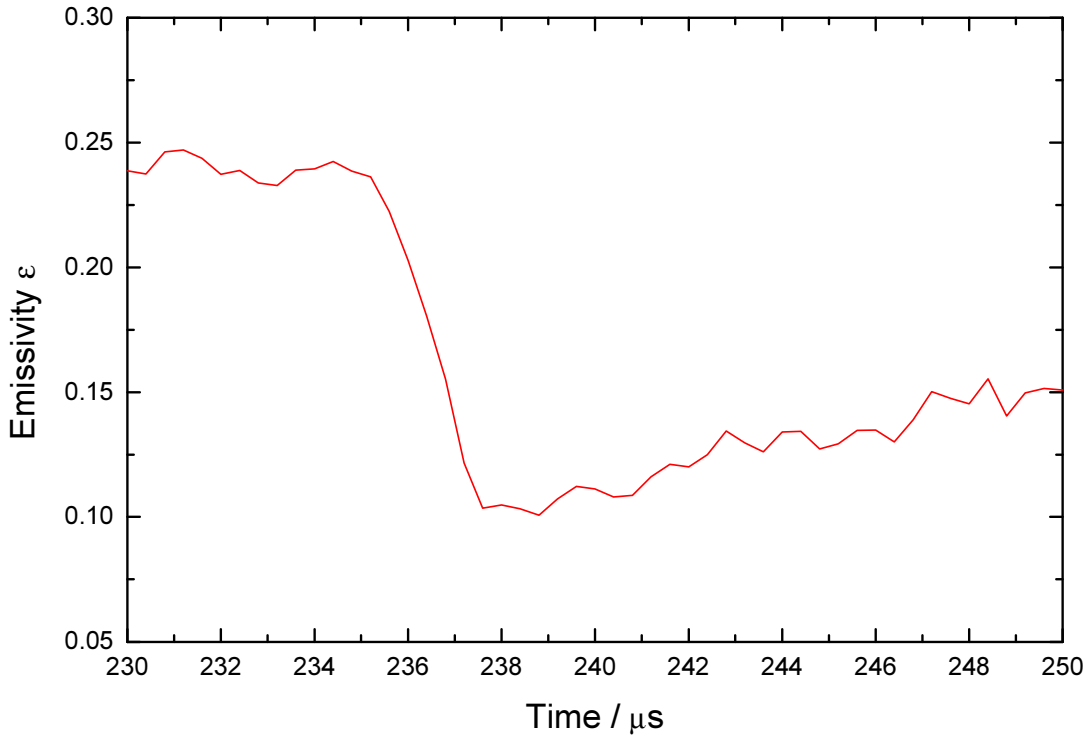

Fig. 17: Emissivity ε of Copper versus time during a pulse-heating experiment. The melting of the wire is between 237 and 240 μs. (Note: Polarimeter measurements are performed at only one wavelength at 684 nm.)

The value for emissivity ε before melting is arbitrary, depending only on the previous preparation of the surface. In Fig.(17) the signal for emissivity decreases strongly as the wire reaches T_m. The literature value for ε at this wavelength is $\varepsilon(T_m) = 0{,}12$, [Krishnan, 1999]. Fig.(17) shows clearly, that our measurement matches this value at the melting temperature T_m. The most interesting fact is, that ε rises again in the liquid phase as temperature increases and reaches a value of 0,15 at 2000 K.

4.5 Experimental parameters and specific values used for calculations

Table 3: Copper specific values and experimental parameters

Specimen material	Copper (Cu)
Manufacturer	Advent Research Materials Ldt. Eynsham, England
Shape	Wire
Diameter	0,5 mm
Purity	99,996 % (non oxygen free)
Hardness	Temper as drawn
Density at 298 K	8960 $kg \cdot m^{-3}$
Melting point	1356 K
Boiling point	2840 K
Specimen length	Variable (45 - 55 mm)
Charging-voltage	6.5 - 7.5 kV
Wavelength λ	1570 nm

Chapter 4

Results

5.1 Experimental results

The experimental parameters for Copper can be seen in Tab.(3). In the temperature range between 1000 K and 2200 K, the following properties are determined from the measured signals:

(i) enthalpy H

(ii) specific heat (under constant pressure) c_P

(iii) electrical resistivity without correction of the volume expansion ρ_0

(iv) volume expansion

(v) electrical resistivity including correction of the volume expansion ρ_{corr}

(vi) thermal conductivity λ

(vii) thermal diffusivity a

Please note, that all graphs in this chapter show these properties versus temperature T. Although graphs property versus enthalpy would be more accurate, it is commonly of more interest for technical use to plot the properties versus temperature. Error bars at significant temperatures (about 1150 K, 1400 K, and 1850 K) are also shown in the graphs.

Enthalpy H

Figure (18) shows enthalpy H versus temperature T. The results of the measurements are given by the following linear polynomial fits of approximately 15 separate measurements. The non-

linear curve during melting is, as we think, a result of surface effects (a change in emissivity) and a slight oscillation of the amplifier-electronic.

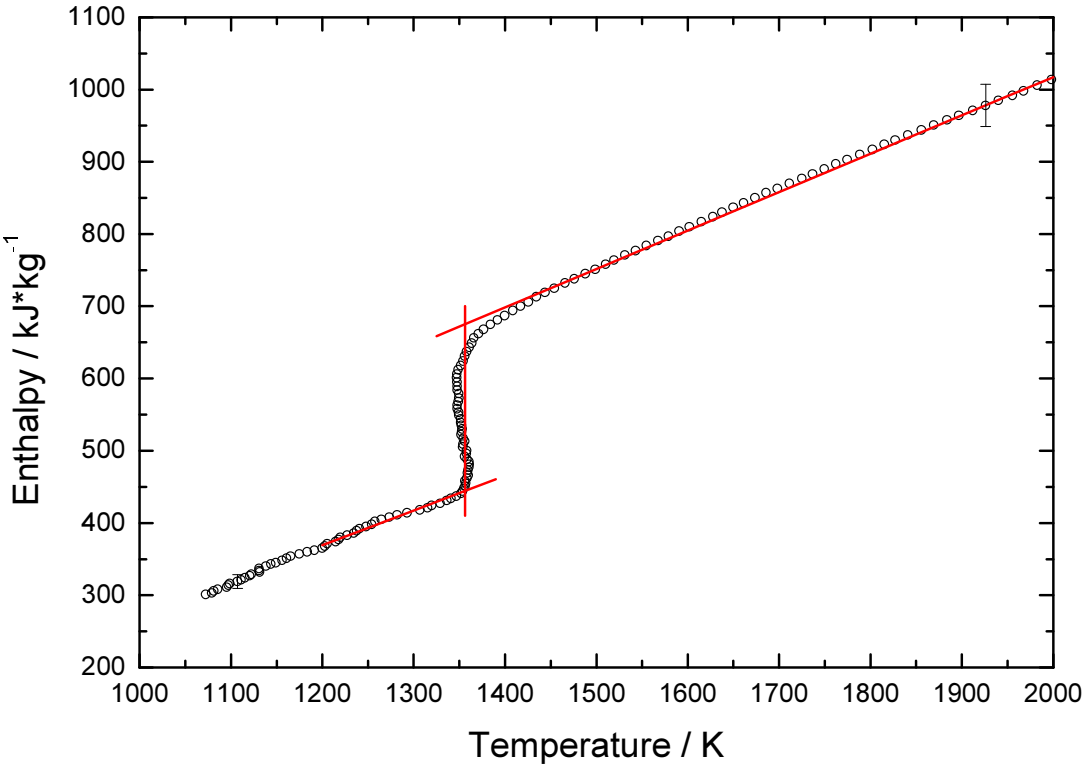

Fig. 18: Specific enthalpy H versus temperature T of Copper. ○ are data points of the measurement, solid lines are the least-squares-fits.

Polynomial fit-results for the enthalpy H(T) in the solid state and in the liquid phase:

	Polynomial fits, H(T) / kJ·kg^{-1}	**Temperature-range of validity**
solid:	H(T) = - 207,894 + 0,4809·T	1100 K < T < 1356 K
liquid:	H(T) = - 45,463 + 0,53145·T	1356 K < T < 2000 K

At the melting-transition, the change in enthalpy ΔH_m is:

$$\mathbf{\Delta H_m = 231\ kJ \cdot kg^{-1}}$$

Specific heat

As mentioned in the last chapter, the specific heat of Copper is derived from the slopes of the linear sections of the enthalpy versus temperature plot. From the polynomial fits of the enthalpy we obtain for the specific heat:

Specimen	$C_{P,Solid}$	$C_{P,liquid}$
Copper-wire	481 $J \cdot kg^{-1}K^{-1}$	531 $J \cdot kg^{-1}K^{-1}$

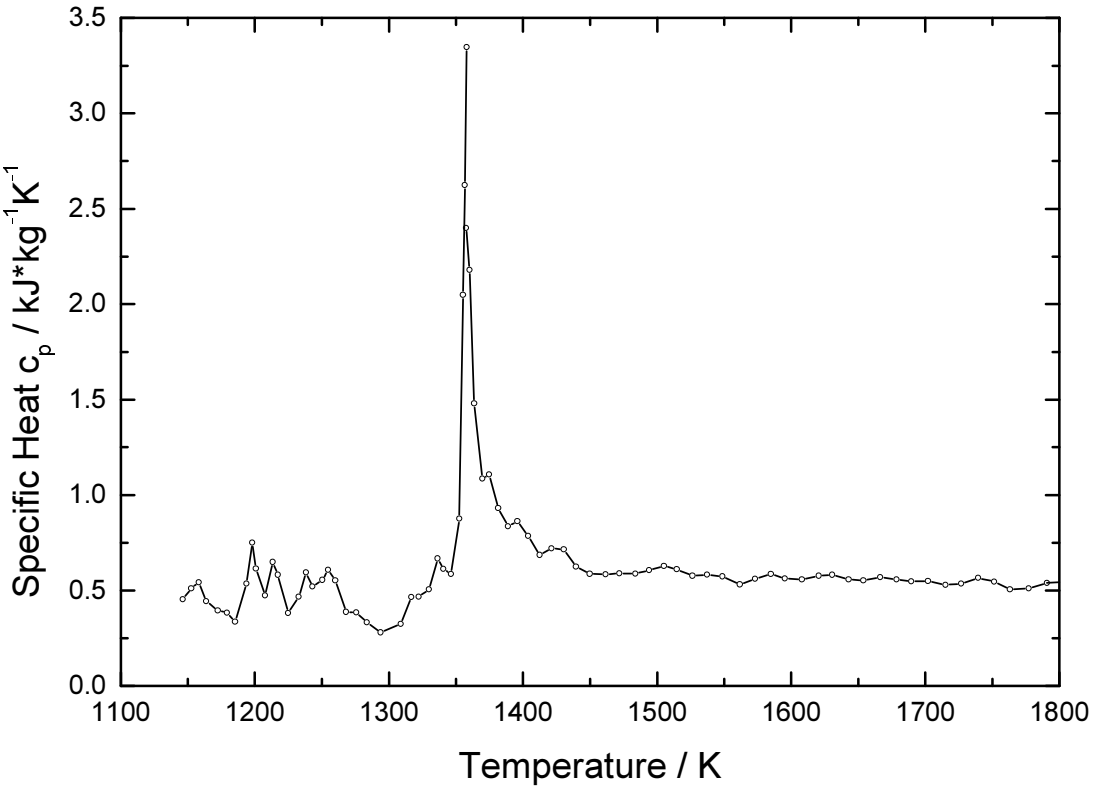

Fig. 19: Specific heat c_P versus temperature T calculated from the enthalpy H with Eq.(4-5).

Note: Fig.(19) is derived from our measurements and not directly measured. Although the values for c_P are not as steady as the ones obtained by a DSC measurement, the plot shows the correct functional form of c_P at the melting-transition.

Electrical resistivity without correction of volume expansion

The electrical resistivity without correction is calculated by using Eq.(4-6):

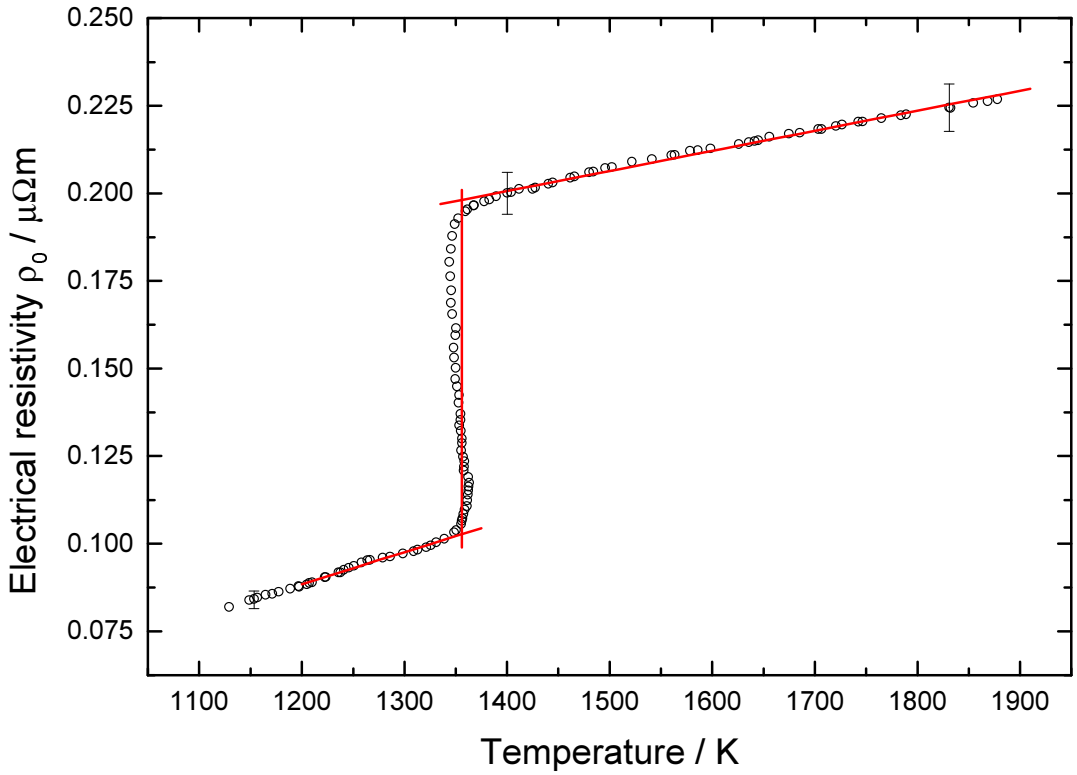

Fig. 20: Electrical resistivity ρ_0 versus temperature T. ○ are data points of the measurement, solid lines are the least-squares-fits.

	Polynomial fits, ρ_0(T) / μΩ·m	**Temperature-range of validity**
solid:	$\rho_0(T) = -0{,}0214 + 9{,}1542 \times 10^{-5} \cdot T$	1100 K < T < 1356 K
liquid:	$\rho_0(T) = 0{,}1092 + 6{,}5009 \times 10^{-5} \cdot T$	1356 K < T < 1900 K

At melting, the change in electrical resistivity without volume correction is:

$$\Delta\rho_0 = \mathbf{0{,}095}\ \mu\Omega\cdot\mathbf{m}$$

Volume expansion

As explained earlier, the volume expansion of Copper has not been measured within this work. Several investigators (e.g. [Nußbaumer, 1993] in our laboratory, or [Gathers, 1983]) have determined reliable and accurate polynomial fits for the volume expansion of pure Copper. We decided to use these data instead of measure it ourselves.

The volume expansion in the solid phase is calculated from linear expansion data for pure Copper published by [Goldsmith, 1961] and [NIST,1990]. Whereas Eq.(5-1), published by [Blumm and Henderson, 1999], was used to derive the volume expansion V/V_0 from linear expansion L/L_0:

$$\frac{\Delta V}{V_0} = 3 \cdot \left(\frac{\Delta L}{L_0} \right) + 3 \cdot \left(\frac{\Delta L}{L_0} \right)^2 + \left(\frac{\Delta L}{L_0} \right)^3 \qquad \textbf{4-1}$$

The best way to fit the calculated data for V/V_0 is a 3rd order polynomial fit shown below.

For the liquid phase we used the polynomial fit from the work of [Nußbaumer, 1993] who determined the volume expansion $V/V_0(H)$. We adapted the polynomial fit and obtained $V/V_0(T)$.

	Polynomial fits, V/V_0	**Temperature-range of validity**
solid:	$V/V_0(T) = 0{,}9907 + 3{,}2232 \times 10^{-5} \cdot T - 4{,}5658 \times 10^{-9} \cdot T^2 + 5{,}2713 \times 10^{-12} \cdot T^3$	$300\ K < T < 1356\ K$
liquid:	$V/V_0(T) = 1{,}0085 + 6{,}3923 \times 10^{-5} \cdot T$	$1356\ K < T < 2000\ K$

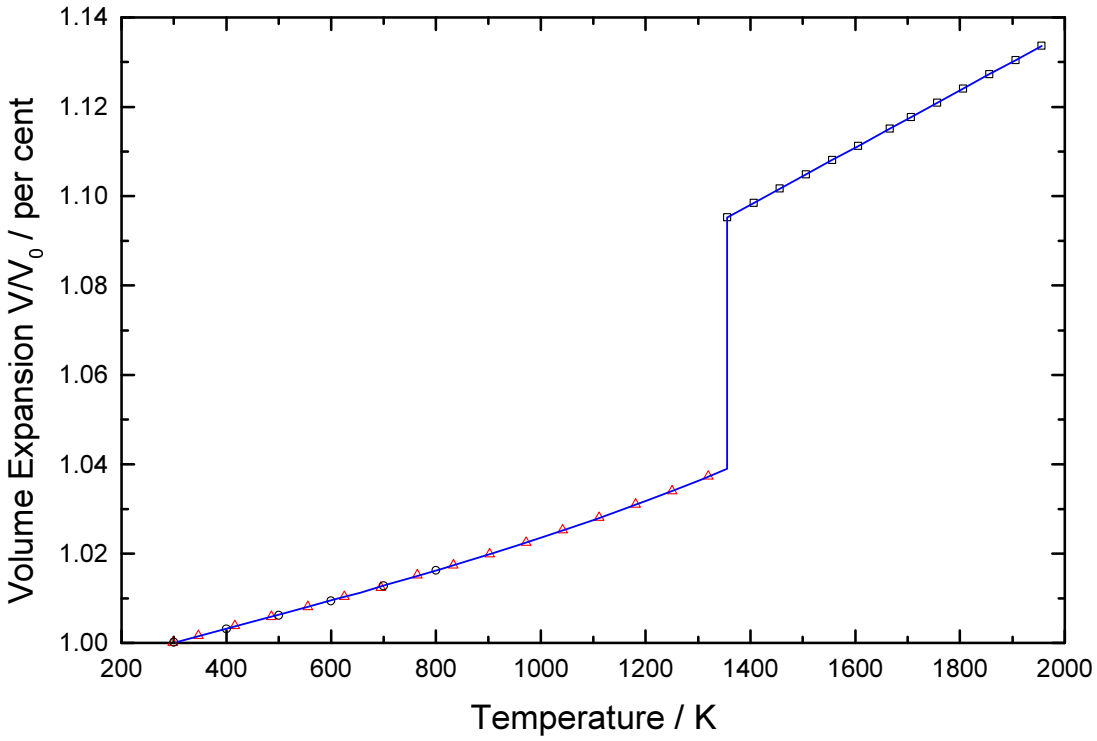

Fig. 21: Volume expansion V/V_0 versus temperature T. △ are values from [Goldsmith, 1961], ○ are [NIST,1990] values and □ represent the values measured by [Nußbaumer, 1993]. The solid line is the polynomial fit for the volume expansion.

For pure metals, several experimental investigations estimated a value for the volume change during melting in the range between 3 - 7 per cent. The change during melting obtained by our polynomial fits is 5,6 %. Literature values for the volume-change at the solid-liquid transition of pure Copper are 5,1 % [Askeland, 1996] and 5,3 % [Blumm, Henderson, 1999]. The actual densities are listed in Tab.(4).

Electrical resistivity with correction of the volume expansion

By using the fits for the volume expansion, one can calculate the volume-corrected electrical resistivity with Eq.(4-7).

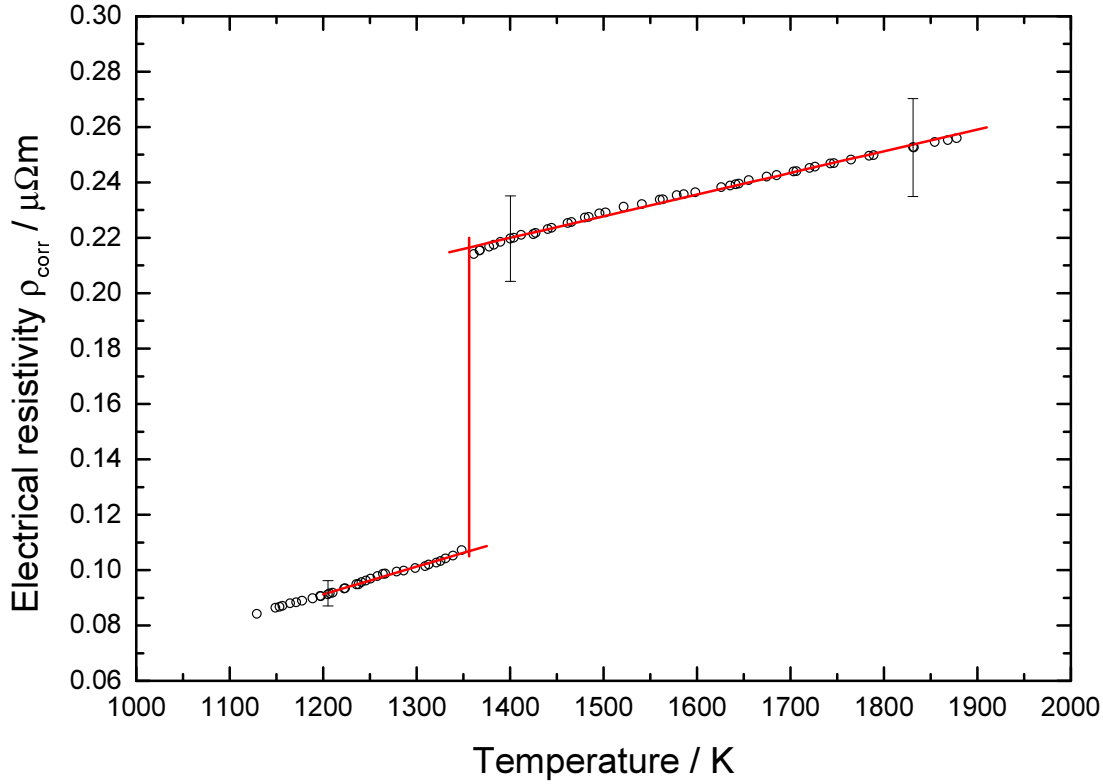

Fig. 22: Volume-corrected electrical resistivity ρ_{corr} versus temperature T.

	Polynomial fits, $\rho_{corr}(T)$ / µΩ·m	**Temperature-range of validity**
solid:	$\rho_{corr}(T) = - 0{,}02861 + 9{,}98873 \times 10^{-5} \cdot T$	$1100\ K < T < 1356\ K$
liquid:	$\rho_{corr}(T) = 0{,}11031 + 7{,}83066 \times 10^{-5} \cdot T$	$1356\ K < T < 1900\ K$

By considering the volume-correction, the change $\Delta\rho_{corr}$ at melting is:

$$\Delta\rho_{corr} = \mathbf{0.109}\ \mu\Omega\cdot\mathbf{m}$$

Thermal conductivity

As shown in Eq.(4-9), thermal conductivity is calculated by using temperature, corrected electrical resistivity, and the LORENTZ number.

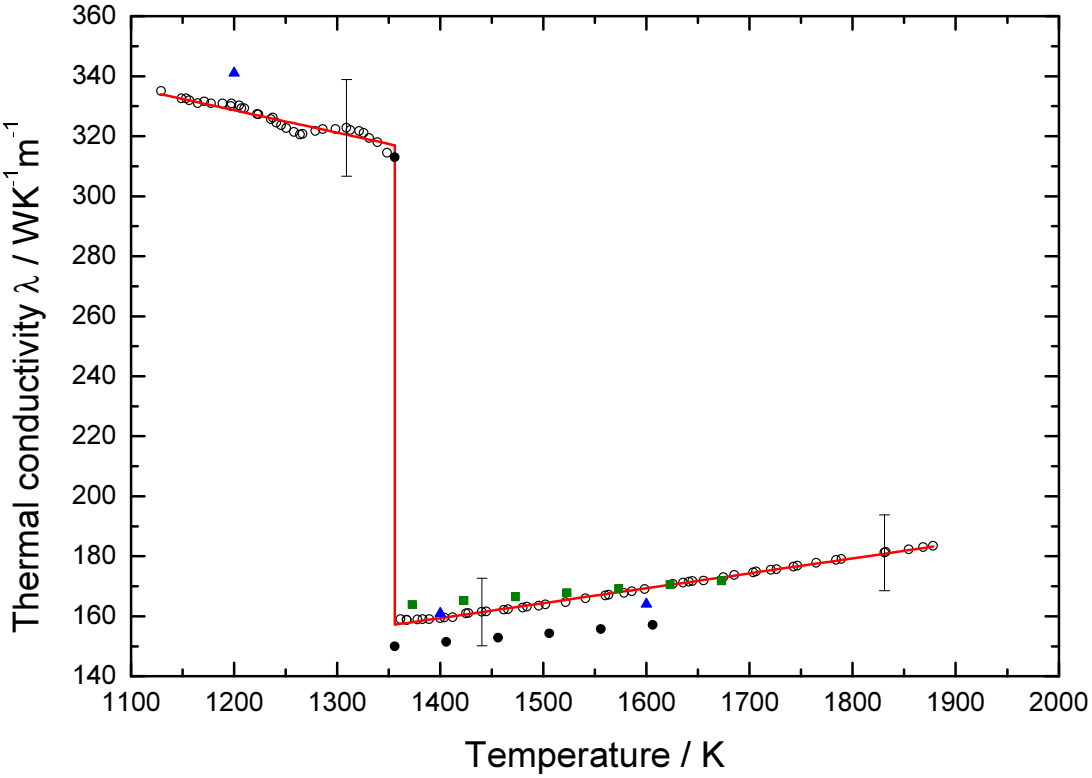

Fig. 23: Thermal conductivity λ versus temperature T. ○ are the measured data points, solid lines are the least-squares-fits, ● are from [Pottlacher, 1999], ■ are from [Zinovyev, 1994], and ▲ are from [Tye, 1979].

The least-squares-fits for the thermal conductivity are:

	Polynomial fits, λ / $W \cdot K^{-1} \cdot m^{-1}$	**Temperature-range of validity**
solid:	$\lambda(T) = 418{,}7775 - 0{,}07509 \cdot T$	$1100\ K < T < 1356\ K$
liquid:	$\lambda(T) = 89{,}7067 + 0{,}04976 \cdot T$	$1356\ K < T < 1900\ K$

Thermal diffusivity

For calculating thermal diffusivity with Eq.(4-10) the density d at a given temperature is needed, which can be obtained by:

$$d(T) = \frac{8960}{\frac{V}{V_0}(T)} \qquad \textbf{4-2}$$

where $V/V_0(T)$ is the relative volume expansion at a given temperature T, and 8960 is the density of Copper in $kg \cdot m^{-3}$ at 298 K.

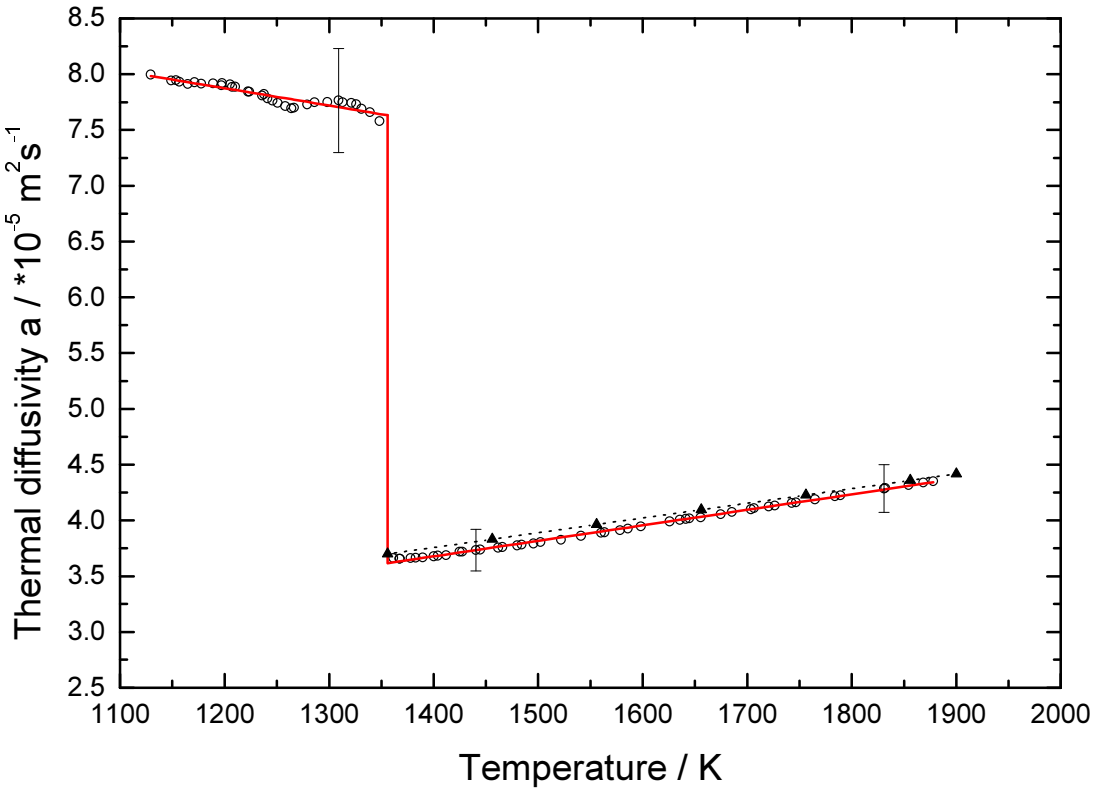

Fig. 24: Thermal diffusivity a versus temperature T. ○ are the data points, the solid line is the least-squares-fit and --▲-- are values from [Cusco, Monaghan, 1999].

Polynomial fits for the thermal diffusivity a(T) for Copper:

	Polynomial fits, a / $m^2 \cdot s^{-1}$	**Temperature-range of validity**
solid:	$a(T) = 9{,}7392 \times 10^{-5} - 1{,}5536 \times 10^{-8} \cdot T$	1100 K < T < 1356 K
liquid:	$a(T) = 1{,}7314 \times 10^{-5} + 1{,}3903 \times 10^{-8} \cdot T$	1356 K < T < 1900 K

5.2 Tabular summary of the experimental results

To sum up the results of this chapter, Tab.(4), which is shown on the next page, lists in the range between 1100 K and 2000 K (in 50 K steps) values for all of the properties calculated from the polynomial fits.

Tab. 4: Thermophysical properties of copper at given temperatures
T - Temperature, H - Enthalpy, ρ_0 - spec. Resistivity (uncorrected), V/V_0 - Volume expansion, d - Density, ρ_{corr} - spec. Resistivity (corrected), λ - Thermal conductivity, *a* - Thermal diffusivity

T **K**	**H** **kJ·kg^{-1}**	ρ_0 **μΩ·m**	**V/V_0**	**d** **kg·m^{-3}**	ρ_{corr} **μΩ·m**	λ **W·K^{-1}·m^{-1}**	***a*** **m^2·s^{-1}**
1100	321.1	0.079	1.028	8719.9	0.081	336.18	8.03 x 10^{-5}
1150	345.1	0.084	1.030	8702.2	0.086	332.42	7.95 x 10^{-5}
1200	369.2	0.088	1.032	8684.0	0.091	328.67	7.87 x 10^{-5}
1250	393.2	0.093	1.034	8665.3	0.096	324.92	7.80 x 10^{-5}
1300	417.3	0.098	1.036	8646.1	0.101	321.16	7.72 x 10^{-5}
1356 s	***444.2***	***0.103***	***1.039***	***8623.8***	***0.107***	***316.96***	***7.63 x 10^{-5}***
1356 l	***675.2***	***0.197***	***1.095***	***8181.3***	***0.216***	***157.18***	***3.62 x 10^{-5}***
1400	698.6	0.200	1.098	8160.4	0.220	159.37	3.68 x 10^{-5}
1450	725.1	0.203	1.101	8136.7	0.224	161.86	3.75 x 10^{-5}
1500	751.7	0.207	1.104	8113.1	0.228	164.35	3.82 x 10^{-5}
1550	778.3	0.210	1.108	8089.7	0.232	166.83	3.89 x 10^{-5}
1600	804.9	0.213	1.111	8066.4	0.236	169.32	3.96 x 10^{-5}
1650	831.4	0.216	1.114	8043.3	0.240	171.81	4.03 x 10^{-5}
1700	858.0	0.220	1.117	8020.3	0.243	174.30	4.09 x 10^{-5}
1750	884.6	0.223	1.120	7997.4	0.247	176.79	4.16 x 10^{-5}
1800	911.1	0.226	1.124	7974.6	0.251	179.27	4.23 x 10^{-5}
1850	937.7	0.229	1.127	7952.0	0.255	181.76	4.30 x 10^{-5}
1900	964.3	0.233	1.130	7929.5	0.259	184.25	4.37 x 10^{-5}
1950	990.9	0.236	1.133	7907.2	0.263	186.74	4.44 x 10^{-5}
2000	1017.4	0.239	1.136	7884.9	0.267	189.23	4.51 x 10^{-5}

5.3 Comparison with literature

Tab. 5: Comparison of enthalpy H, specific heat cp, and electrical resistivity ρ with literature data. (subscripts: $_s$ indicates solid state values, $_l$ values in the liquid phase, and $_{s-l}$ values at the solid-liquid transition; Note: * indicates non volume-corrected values)

H_s	H_l	ΔH_{s-l}	$c_{p,s}$	$c_{p,l}$	ρs	ρ_l	$\Delta\rho_{s-l}$	Reference
444	675	231	481	531	0.107	0.216	0.109	this work
463	665	202	-	532	0.106*	0.222	0.116	[Nußbaumer, 1993]
470	700	230	-	-	-	-	-	[Gallob, 1979]
-	671	-	-	-	-	0.215	-	[Gathers, 1983]

Tab. 6: Comparison of thermal conductivity λ and thermal diffusivity *a* with literature data. (Note: $^+$ indicates values at 1300 K.)

λ_s	λ_l	a_s	a_l	Reference
317	157	7.63×10^{-5}	3.62×10^{-5}	this work
313	150	-	-	[Pottlacher, 1999]
-	-	-	3.69×10^{-5}	[Cusco, 1999]
330	160	-	-	[Zinovyev, 1994]
330	163	-	-	[NPL report, 1997]
335^+	-	$7.4 \times 10^{-5+}$	-	[Touloukian, 1967]

Within our estimated uncertainty, all of the given literature data show an excellent agreement for thermal conductivity and thermal diffusivity of Copper.

Chapter 5

Estimation of uncertainty

These following paragraphs are dealing with the problem of determining the accuracy of our results and the belonging errors. Beforehand, it has to be said, that most of the known systematic errors are compensated during the data evaluation, whereas the unknown systematic errors of our measurements are not included within the given uncertainty ranges. The deviation of the own result from proven literature data is a good indicator for the systematic error. Since our results correspond quite well with literature data and recommended values, we think that we have canceled out most of these errors. The stated uncertainties cover the accidental errors which may and do arise during the measurements and the evaluation processes. (Note: subscripts s and l denote solid state-, liquid phase properties)

The current signal: Two different errors can occur within the current measurement. Pearson electronics calibrate their current-probes and guarantee a maximal deviation of ± 0,5 %. The second uncertainty is the signal digitalization within the data registration of the computer. We have 12-bit data-acquisition cards whereas the error is at most in the last digit, hence less than ± 0,5 %. A third - but negligible - point is the uncertainty of the ohmic voltage dividers because of its small contribution of less than 0,1 %. (The same applies to the voltage measurement.) The total error of the current measurement is:

$$\underline{\Delta I = \pm 1\ \%}$$

The voltage signals: The error of the voltage signals is more difficult to estimate than the one of the current signal. The voltage is calculated by Eq.(4-1). As said earlier, the third term dL/dt can be omitted because it is a small contribution to the overall value, but this leads to a small uncertainty. Another error can occur, if the correction of the second term, L·dI/dt, in the same equation is not done accurately. (For some other materials, the voltage signals are not very sensitive on the size of this correction, but with Copper, this correction should be done as

accurate as possible.) Another problem while using these high currents could be the arising skin effect. Earlier estimations have shown, that this influence could be neglected without affecting the signals too much. And as a last point, the voltage measurement is affected by the same digitalization problem as the current signals. If all of the above errors are estimated with ± 0,5 % and are summed up, the total error of the voltage measurement is:

$$\underline{\Delta U = \pm 2\ \%}$$

The temperature measurement: There are mainly two different reasons, that are responsible for an uncertainty of the temperature measurement. First, the interference filter in the pyrometer has a bandwidth of 80 nm while the formalism for calculating the temperature uses an exact wavelength. Simulations from [Sachsenhofer, 2000] showed, that the error is at least less than ± 0,2 %. The second error occurs by setting the ratio of the emissivities $\varepsilon/\varepsilon_m = 1$. We were able to show that the emissivity of Copper slightly rises while overheating the liquid metal. But simulations including this change in emissivity [Seifter, 1996] showed that this forced error is negligible. New simulations for Copper lead at 2000 K to an error less than 0,5 %. Therefore, the total error of the temperature measurement is given by:

$$\underline{\Delta T = \pm 1\%}$$

The mass of the wire: The mass is calculated by the density and the volume of the wire sample, whereas the volume itself has to be calculated from the length of the wire and the diameter. Since the wire is drawn and its diameter is controlled throughout the whole process, the uncertainty of the diameter can be omitted. The only error we can estimate is an uncertainty within the length determination. The length of the wire can be measured with an error of ± 0,1 mm. Considering an average length of the wires of 50 mm, the error is ± 0,5 %. Thus, the error of the mass is also:

$$\underline{\Delta m = \pm 0{,}5\ \%}$$

The enthalpy: The enthalpy is first calculated from the measured values by using Eq.(4-3). The error of H is calculated by summing up the errors of each of the signals used to calculate H. Thus, the total error is ± 3 %. But the calculated error of H is always less than three per cent,

because we average several enthalpy-curves to minimize the statistic errors. Nevertheless, we decided to set the error for the enthalpy to:

$$\underline{\Delta H = \pm 3\ \%}$$

The specific heat: Since the specific heat is calculated from the slope of the linear sections of the enthalpy curve, the error can only be approximated statistically. The error of the specific heat is the uncertainty of the slope of the linear fit. Since there are more (and even more accurate) data points for calculating the linear fit of the liquid phase, $c_{P,l}$ is more accurate than $c_{P,s}$. The errors for the specific heat are:

$$\underline{\Delta c_{P,s} = \pm 2\ \%}$$

$$\underline{\Delta c_{P,l} = \pm 1\ \%}$$

The uncorrected electrical resistivity: The same points - as said before while handling the error of the enthalpy - are applying to ρ_0 as well. Thus the uncertainty is the same:

$$\underline{\Delta \rho_0 = \pm 3\%}$$

The volume expansion: Since we used literature data for the volume expansion, we have to use error estimations. The volume expansion data for the solid state are very accurate and often proved by different measurements, so the estimated value for the uncertainty is ± 2 %. For the liquid phase, we used a polynomial fit which was measured in our own laboratory and whose uncertainty was determined to ± 4 %. As a result, we have for the error of the volume expansion:

$$\underline{\Delta V/V_{0,s} = \pm 2\ \%}$$

$$\underline{\Delta V/V_{0,l} = \pm 4\ \%}$$

The corrected electrical resistivity: ρ_{corr} is calculated from the uncorrected electrical resistivity and the volume expansion. Therefore, the errors of both quantities are summed up and result in the total uncertainty of ρ_{corr}, which is:

$$\underline{\rho_{corr,s} = \pm 5\ \%}$$

$$\underline{\rho_{corr,l} = \pm 7\ \%}$$

The thermal conductivity: This quantity is calculated by using Eq.(4-9). The biggest problem while handling this equation is the error-estimation of the LORENTZ-number L, since the values reported for L are varying in the range between 2,45 and 2,60 x 10^{-8} V^2/K^2. We decided to regard L as a constant which has the error zero, because if anyone is able to determine the correct value of L for Copper, we will use it for our calculations and are able to change our results immediately. Therefore, the total error of λ consists of the errors of the temperature and the corrected electrical resistivity. By following the rules of the basic error-propagation calculations, one gets:

$$\frac{\Delta\lambda}{\lambda} = \frac{\Delta T}{T} + \frac{\Delta\rho_{corr}}{\rho_{corr}} \qquad \textbf{5-1}$$

Since the determination of both quantities is independent from the other, we can rearrange this equation and obtain:

$$\frac{\Delta\lambda}{\lambda} = \sqrt{\left(\frac{\Delta T}{T}\right)^2 + \left(\frac{\Delta\rho_{corr}}{\rho_{corr}}\right)^2} \qquad \textbf{5-2}$$

If this calculation is carried out, one gets for the total uncertainty of the thermal conductivity:

$$\underline{\Delta\lambda_S = \pm 5\ \%}$$

$$\underline{\Delta\lambda_l = \pm 7\ \%}$$

The thermal diffusivity: Last but not least, we have to deal with the uncertainty of thermal diffusivity which is calculated by using Eq.(4-10). For calculating the error of this quantity, it is necessary to rearrange the equation to see that thermal diffusivity is independent from the volume expansion:

$$a = \frac{\lambda}{c_p \cdot d} = \frac{\dfrac{L \cdot T}{\rho_0 \cdot V/V_0}}{c_p \cdot \dfrac{d_0}{V/V_0}} = \frac{L \cdot T}{\rho_0 \cdot c_p \cdot d_0} \neq a\left(\frac{V}{V_0}\right) \qquad \textbf{5-3}$$

Otherwise, the volume expansion V/V_0 would be considered twice and the error would become erroneously large. By applying the same formalism as for thermal conductivity to Eq.(6-3), one gets (since L and d_0 are constants):

$$\frac{\Delta a}{a} = \frac{\Delta T}{T} + \frac{\Delta \rho_0}{\rho_0} + \frac{\Delta c_p}{c_p} \qquad \textbf{5-4}$$

The only difference between the error-calculation of thermal conductivity and diffusivity is, that the different terms of Eq.(6-4) are not independent from each other and must not be summed up geometrically. By calculating the total error of thermal diffusivity, one obtains:

$$\underline{\Delta a_s = \pm 6\ \%}$$

$$\underline{\Delta a_l = \pm 5\ \%}$$

Tabular summary of this chapter

Tab. 7: Measured and calculated properties of Copper with their belonging errors
solid state: 1100 K < T < 1356 K, liquid phase: 1356 K < T < 2000 K

	Error	
Quantity	**solid state**	**liquid phase**
Current I	± 1 %	
Voltage U	± 2 %	
Temperature T	± 1 %	
Mass m	± 0,5 %	
Enthalpy H	± 3 %	
ΔH_m	± 6 %	
Specific heat c_P	± 2 %	± 1 %
uncorr. Resistivity ρ_0	± 3 %	
Volume expansion V/V_0	± 2 %	± 4 %
Density d	± 2%	± 4 %
corr. Resistivity ρ_{corr}	± 5 %	± 7%
$\Delta\rho_{corr}$	± 12 %	
therm. Conductivity λ	± 5 %	± 7 %
therm. Diffusivity a	± 6 %	± 5 %

Chapter 6

Conclusion and outlook

The thermophysical properties of Copper up to 500 K into the liquid phase have been measured within the current work by using an ohmic pulse-heating technique. Among these properties are two, which were of particular interest: thermal conductivity and thermal diffusivity.

As a first point, we showed that our pulse-heating apparatus can be adapted for measurements on low melting metals without expanding the uncertainty of the experimental data. We are able to show that our values for enthalpy, electrical resistivity and specific heat - in the solid state as well as in the liquid phase - correspond very well with literature data within the uncertainty ranges. We used the WIEDEMANN-FRANZ-LORENTZ law to determine thermal conductivity and thermal diffusivity. Normally, these properties are measured directly, as shown in most publications, by using e.g. a laser flash apparatus. Our obtained results are in excellent agreement with literature values (i.e. [Cusco, 1999]), although we calculated these properties.

As a future project, accurate emissivity measurements with our DOAP system should be performed on Copper for various reasons:

(i) further testing of the DOAP system
(ii) minimization of the uncertainty of the temperature in the liquid phase
(iii) basic research reasons

Particularly, (ii) is of great interest for our measurements with regard to make the results as accurate as possible. As mentioned before, (iii) should be also of great interest, because the emissivity ε for Copper seems to rise again in the liquid phase as temperature increases.

Several years ago, we were able to determine with our apparatus the properties of Gold [Nußbaumer, 1993]. Now we applied - with equally success - the pulse-heating technique to Copper and were also able to add thermal conductivity/diffusivity to the determined properties. Therefore the next logical step should be to figure out, if we are able to expand our measurements to the next lower-melting metal: Silver.

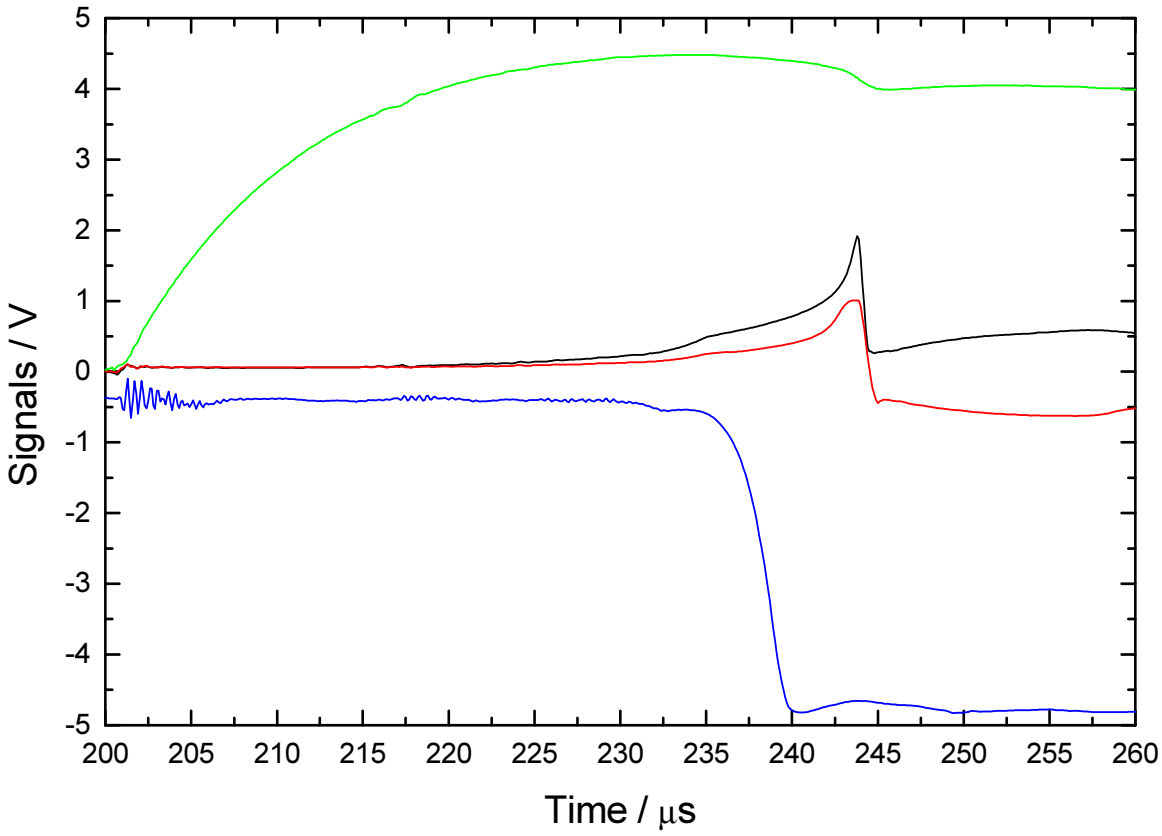

Fig. 25: The detected signals of Silver. Signals: green: current; red, black: voltage; blue: surface radiance The horizontal, linear section of the radiance signal between 232 and 235 µs indicates the melting of the wire.

Fig.(25) - as a first attempt - clearly shows the melting plateau of Silver (T_m = 1234 K) time resolved together with all the other electrical signals. This first and very encouraging experiment on Silver should be used as a starting point for measurements on Silver as a future project. These measurements would not only be a further test for the abilities of the pyrometer, but also very challenging, because up to now, no accurate measurements on Silver have been performed with the pulse-heating technique.

Chapter 7

References

Askeland D. R., 1996: *Materialwissenschaften*, Spektrum Verlag GmbH, Heidelberg, p.203.

Bergmann L., Schaefer C., 1990: *Lehrbuch der Experimentalphysik, Band I, 10.Auflage,* Walter de Gruyter, New York.

Blumm J., Henderson J. B.,1999: *Measurement of the Volumetric Expansion and Bulk Density of Metals in the Solid and Molten Regions*, presented at the 15th ETCP, Würzburg, Germany.

Bronstein I. N. - Semendjajew K. A., 1991: *Taschenbuch der Mathematik, 25.Auflage,* B. G. Teubner, Stuttgart.

Cusco L., Monaghan B. J., 1999: *UK national standard for the thermal properties of molten materials: thermal diffusivity of molten copper*, presented at the 15th ETCP, Würzburg, Germany.

Gallob R., 1979: *Messung thermophysikalischer Daten von flüssigem Nickel und Kupfer mit Hilfe der Drahtexplosionsmethode*, Diplomarbeit.

Gathers G. R., 1983: *Thermophysical Properties of liquid Copper and Aluminium,* International Journal of Thermophysics, Vol.4, p. 209-226.

Goldsmith A., Waterman T. E., Hirschhorn H .J., 1961: *Handbook of Thermophysical Properties of Solid Materials: Volume I – Elements*, Pergamon Press, Oxford.

Hultgren R., Desai P. D., Hawkins D. T., Gleiser M., Kelley K.K. and Wagman D. D., 1973: *Selected Values of thermodynamic Properties of the Elements*, American Society for Metals.

Klemens P. G. and Williams R. K., 1986: *Thermal conductivity of metals and alloys*, International Metals Reviews, Vol.31, No.5, p. 197-215.

Krishnan S., 1999: private communication.

Maglić K. D., Cezairliyan A. and Peletsky V. E., 1982: *Compendium of Thermophysical Property Measurement Methods,* Volume 2, Plenum Press, New York.

Maglić K. D., Cezairliyan A. and Peletsky V. E., 1984: *Compendium of Thermophysical Property Measurement Methods,* Volume 1, Plenum Press, New York.

Mills K. C., Monaghan B. J. and Keene B. J., 1997: *Thermal Conductivities of Molten Metals, Part 1 - Pure Metals*, NPL Report CMMT(A) 53.

National Institute of Standards and Technology (NIST), 1990: *Certificate of Standard Reference Material 736 (Copper Thermal Expansion)*, Standard Reference Materials Program.

Nussbaumer, G., 1993: *Weiterentwicklung der zeitaufgelösten Expansions- und Spannungs-messung bei Mikrosekunden - Pulsheizexperimenten. Bestimmung thermophysikalischer Daten von Kupfer und Gold*, Diplomarbeit

Pottlacher G., 1998: *Beiträge zur experimentellen Untersuchung thermophysikalischer Daten flüssiger Metalle und Legierungen,* Habilitationschrift.

Pottlacher G., 1999: *Thermal conductivity of pulse-heated liquid metals at melting and in the liquid phase*, Journal of Non-Crystalline Solids 250-252, p. 177-181.

Sachsenhofer F., 2000: *Data evaluation for pulse heating experiments combined with emissivity measurements using a division-of-amplitude photopolarimeter,* Diplomarbeit.

Seifter A., 1996: *Bestimmung thermophysikalischer Daten von Eisen-Nickel-Legierungen im flüssigen Zustand mittels ohmscher Pulsaufheizung,* Diplomarbeit.

Speyer R. F., 1994: *Thermal Analysis of Materials*, Marcel Dekker, Inc., New York.

Touloukian Y. S., 1967: *Thermal Properties of High Temperature Solid Materials, Vol. 1: Elements*, p. 458-462, The MacMillan Company, New York.

Tye R. P., Hayden R. W., 1979: *The thermal conductivity and electric resistivity of copper and copper alloys in the molten state*, High Temperatures - High Pressures, Vol. 11, p. 597-605.

Weißmantel Ch. und Hamann C., 1990: *Grundlagen der Festkörperphysik,* 7.Auflage, Springer Verlag, Berlin.

Zinovyev V. E., Taluts S. G., Kamashev M. G., Vlasov B. V., Polykova V. P., Korenovskii N. I., Chipina L. I., Zagrebin L. D., 1994: *Thermal Properties and Lorentz Numbers of Copper and Silver at High and Average Temperatures*, Phys. Met. Metall. 77, p.492-497.

Die vorliegende Arbeit wurde am Institut für Experimentalphysik der Technischen Universität Graz unter der Leitung von Herrn a.o. Univ.- Prof. Dr. Gernot Pottlacher durchgeführt. Ihm gebührt meine vollste Hochachtung und sei an dieser Stelle mein ganz besonders Dank ausgedrückt: Nicht nur für die Bereitstellung der apparativen Mittel zur Durchführung dieser Arbeit, sondern auch für so viele andere Dinge, daß eine vollständige Auflistung den Rahmen dieser Seite sprengen würde. Seine Hilfsbereitschaft war so groß, daß er auch in seiner Freizeit noch Zeit für mich erübrigte und immer ein gutes Wort oder einen guten Vorschlag parat hatte. Ohne sein Zutun wäre diese Arbeit nie zustande gekommen.

Ebenso zu Dank verpflichtet fühle ich mich meinen beiden Freunden und Kollegen DI Achim Seifter und Franz Sachsenhofer. Sie sind mir während der Arbeit nicht nur mit sehr zahlreichen und wertvollen Ratschlägen zur Seite gestanden, sondern halfen mir auch immer wieder aus experimentellen Sackgassen. Außerdem sorgten sie neben der Arbeit für ein wirklich angenehmes Klima und den nötigen Spaß im Labor.

Da während meiner Diplomarbeit der Institutsvorstand wechselte, möchte ich mich bei beiden Vorständen, Herrn Univ.-Prof. Dr. Helmut Jäger und Herrn a.o Univ.-Prof. Dr. Laurentius Windholz, herzlich bedanken, sowie bei all den anderen ungenannten Mitgliedern des Institutes für die Hilfsbereitschaft und das angenehme Arbeitsklima.

Für all die Freundschaft und die schönen Momente während des Studiums möchte ich auch meine Studienkolleginnen und Kollegen danken, die mir stets halfen den richtigen Weg durch die "Untiefen" der Physik zu finden.

Zu guter Letzt sei an dieser Stelle meinen Eltern, Geschwistern, Verwandten und Freunden gedankt, die mich während des Studiums unterstützt haben, auch wenn sie sich nicht immer genau vorstellen konnten, was ich gerade mache. Mein ganz besonderer Dank gilt aber meiner Freundin Angelika: Sie war wirklich immer für mich da und mußte auch öfters meinen Mißmut nach Fehlschlägen ertragen.

DANKE !